Ocean Engineering 241 (2021) 110033

Contents lists available at ScienceDirect

Ocean Engineering

journal homepage: www.elsevier.com/locate/oceaneng

Hydrodynamic force acted on a solid translating in nonuniform stream ☆

Xianwu Lin *, Lixun Xiong

School of aerospace engineering, Xiamen University, 361102, China

ARTICLE INFO

Keywords:
Hydrodynamic force
Incompressible flow
Panel method
Uniform velocity gradient stream

ABSTRACT

To predict the effect of the uniform gradient stream, the hydrodynamic force acting on a translating solid is studied following the Newman method. Some new hydrodynamic force formulas that are valid in both two-dimensional and three-dimensional flow are proposed. A new and efficient velocity-vector based method is proposed to compute the added mass that is required in the new formulas. Abundant numerical examples are designed to check the correctness of the new formulas and the validity of the Newman hypothesis adopted during the proof. Comparison with classical results shows that the formula proposed by Taylor and Newman are only two special cases of the present study. Comparison with some recent studies are also studied and their rationality is analyzed.

1. Introduction

The study on the hydrodynamic force acted on a solid moving in a non-uniform stream has a significant meaning in engineering. Many aircrafts like airship (Mueller et al., 2009; Wang et al., 2020), quadrotor (Escareno et al., 2013), bionics flapping aerocraft (Sun, 2014) fly with speed comparable with the wind. Many underwater vehicles like submarine (Kunze et al., 2002), remote operation vehicle (Shen and Hou, 2016) or offshore structures (Faltinsen, 1990; Agarwal and Jain, 2003; Zan and Lin, 2020) are susceptible to the ocean internal waves. To better understand the dynamical behavior of these objects and control them validly, it is necessary to evaluate the hydrodynamic forces acted on them first. These hydrodynamic forces can of course be acquired by experiment or CFD technology. However, these methods would be expensive or time-consuming as the wind or ocean internal wave is often non-uniform and the test or computation should be carried out under different stream velocity gradients. The analytical formula that can estimate the effect on the hydrodynamic force by the stream velocity gradient would drastically reduce the experimental cost or computing time. To study the character of the ocean's internal wave, the underwater glider is often employed (Fan and Woolsey, 2014). By measuring the position and velocity of the glider, the parameters describing the internal wave, including the velocity gradient can be estimated. The accuracy of this estimation is dependent on the accuracy of the glider motion model in which the effect of the stream velocity gradient on the hydrodynamic force should be analytically described. In a wind tunnel or water tunnel experiment, the section area is varying due to the displacement thickness of the boundary layer. In this case, the undisturbed flow field before the vehicle model is put in would be nonuniform. Consequently, theoretical prediction on the effect of the stream gradient is required to revised experimental data and improve the tunnel test accuracy (Taylor, 1928). All the requirements listed above show the necessity to study the effect on a solid's hydrodynamic force by the stream gradient.

The first systematically studied on this topic is by Taylor (1928) and Lamb (1945) who proposed a hydrodynamic force formula for a solid resting in a steady stream with uniform velocity gradient in 1928. Comparing with the previous work by Thomson (1872) and Munk (1923), Taylor's formula is valid not only for a sphere but also for arbitrary formed solid and arbitrary tensor of the stream gradient. Taylor's formula is confined to the case that the flow is steady. Almost half a century later was the hydrodynamic force formula for unsteady flow introduced in a special way. In 1977, Newman (2017) proposed a formula that predicts the hydrodynamic force acted on an axisymmetric body translating with zero attack angle in the uniform velocity gradient and steady stream. In 2000, Thomasson (2000) further extended Taylor's theory to the case that the stream is unsteady and non-uniform and the solid may translate as well as rotate. Later, this work was revised by Woolsey (2011) and himself (Thomasson and Woolsey, 2013) and is extended to the case that the stream may be rotational. There is something strange in the progress reviewed above. Firstly, the Newman hydrodynamic force formula is not compatible with the Taylor hydrodynamic force formula as the latter is applicable in the case that the solid is not axisymmetric. Secondly, none of the formulas introduced above had been verified by a numerical example. Thirdly,

☆ This work is supported in part by the National Natural Science Foundation of China under Grant No. 61733017 and 61873219.
* Corresponding author.
E-mail addresses: linxianw@xmu.edu.cn (X. Lin), 515142858@qq.com (L. Xiong).

https://doi.org/10.1016/j.oceaneng.2021.110033
Received 16 July 2021; Received in revised form 1 September 2021; Accepted 15 October 2021
Available online 1 November 2021

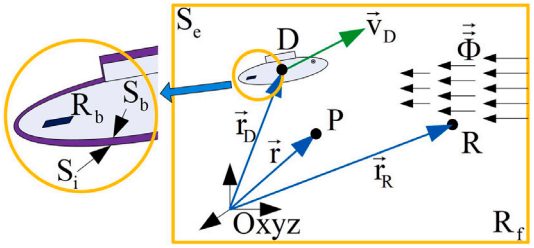

Fig. 1. The relationship of position vectors, surfaces and regions.

all the study reviewed above is focused on three-dimensional flow and no corresponding result in two-dimensional flow had been involved.

Recently, Lin et al. (2021) studied the relative motion principle which can covert the hydrodynamics prediction problem in the unsteady stream into the steady stream case. Consequently, only the hydrodynamics prediction problem for a solid moving in the steady stream need to be studied. The purpose of this study is to provide some hydrodynamic force formulas that are compatible with those of both Taylor and Newman. Attention is paid to the derivation process so that the formulas are valid in both two and three-dimensional flow. In the meantime, a numerical method for evaluating the added mass and the hydrodynamic force is introduced to verify the new formulas. The remaining part of this paper is organized as follows. Section two replaces the velocity-potential in Newman's method with velocity-vector by DMT(Derivative moment transformation) (Wu et al., 2015) formulas and extended Newman's formula to the case that solid is not axisymmetric. Section three verify the newly acquired formulas with abundant numerical examples in both two and three-dimensional flows. Section four compares the newly acquired formulas with the existing result as well as their derivation process. Section five concludes the paper with some remarks. For the completeness of the paper, some vector identities are listed in the appendix as well as the necessary proof.

2. Mathematical formulation

2.1. Description of the flow field

2.1.1. Description of the frames and notations

To describe the motion of the fluid and the solid, an inertial frame $Oxyz$ is built with three base vectors $\mathbf{i},\mathbf{j},\mathbf{k}$. For an arbitrary point P in the flow field, its position vector referencing to O is denoted by $\mathbf{r}$. The solid does not rotate and its translating velocity can be represented by the velocity $\mathbf{v}_D$ of a characteristic point D on the solid. For inviscid flow, the slip boundary condition shows that the velocity on the body surface S_b is different from the corresponding point on the neighboring fluid surface S_i. The region enclosed by S_b is denoted by R_b, the region enclosed S_i is denoted by R_b' as shown in Fig. 1. The region enclosed by S_b and S_i is $R_b'-R_b$ and is called the slip boundary layer. An enclosed surface S_e is drawn in the flow field so that it contains the solid and its surrounding fluid. The region enclosed by S_b and S_e is denoted by R_f, the region enclosed by S_i and S_e is denoted by R_f'. The normal $\mathbf{n}$ on S_e and S_i are pointing outside of R_f' and the normal on S_b is point inside R_b.

The concept of a vector is different from its corresponding column matrix projected in a given frame. The operation of vectors contains dot-product '·' and cross-product '×' but not transposition. The operation of matrixes, however, contains transposition or inversion but not dot product or cross product. The notation of a vector and its corresponding column matrix are both denoted by a boldface letter in many journals. Consequently, one should recognize a boldface letter according to the operator adopted. This notation method is also applied for dyads or tensors in this study.

2.1.2. Description of the stream

Suppose that the stream is steady and the velocity gradient is uniform nearby the solid. In this case, the stream velocity can be expressed as

$$\mathbf{v}_s(\mathbf{r}) = \mathbf{v}_s(\mathbf{r}_R) + (\mathbf{r}-\mathbf{r}_R)\cdot\boldsymbol{\Phi} \tag{1}$$

where $\mathbf{r}_R$ is a reference point on which the stream velocity $\mathbf{v}_s(\mathbf{r}_R)$ is given. $\boldsymbol{\Phi} \doteq \nabla\mathbf{v}_s = \text{const}$ is the gradient of the steam velocity and its matrix in the inertial frame is

$$\boldsymbol{\Phi} = \begin{bmatrix} \frac{\partial v_{s,x}}{\partial x} & \frac{\partial v_{s,x}}{\partial y} & \frac{\partial v_{s,x}}{\partial z} \\ \frac{\partial v_{s,y}}{\partial x} & \frac{\partial v_{s,y}}{\partial y} & \frac{\partial v_{s,y}}{\partial z} \\ \frac{\partial v_{s,z}}{\partial x} & \frac{\partial v_{s,z}}{\partial y} & \frac{\partial v_{s,z}}{\partial z} \end{bmatrix} \doteq \begin{bmatrix} \phi_{11} & \phi_{12} & \phi_{13} \\ \phi_{21} & \phi_{22} & \phi_{23} \\ \phi_{31} & \phi_{32} & \phi_{33} \end{bmatrix} \tag{2}$$

For incompressible flow $\nabla\cdot\mathbf{v}_s = 0$ which means $\frac{\partial v_{s,x}}{\partial x}+\frac{\partial v_{s,y}}{\partial y}+\frac{\partial v_{s,z}}{\partial z} = 0$ or $\phi_{11}+\phi_{22}+\phi_{33} = 0$. It is supposed that the stream is irrotational. In this case $\nabla\times\mathbf{v}_s = 0$ and $\boldsymbol{\Phi}$ is symmetric, i.e., $\phi_{21}=\phi_{12},\phi_{31}=\phi_{13},\phi_{32}=\phi_{23}$. For convenience, three vectors $\boldsymbol{\phi}_x,\boldsymbol{\phi}_y,\boldsymbol{\phi}_z$ is also defined with

$$\boldsymbol{\phi}_x = \begin{bmatrix}\phi_{11}\\ \phi_{12}\\ \phi_{13}\end{bmatrix},\ \boldsymbol{\phi}_y = \begin{bmatrix}\phi_{21}\\ \phi_{22}\\ \phi_{23}\end{bmatrix},\ \boldsymbol{\phi}_z = \begin{bmatrix}\phi_{31}\\ \phi_{32}\\ \phi_{33}\end{bmatrix} \tag{3}$$

It is obvious that $\boldsymbol{\Phi} = \mathbf{i}\boldsymbol{\phi}_x+\mathbf{j}\boldsymbol{\phi}_y+\mathbf{k}\boldsymbol{\phi}_z$.

2.1.3. Description of the disturbed flow field

According to the study of Newman (2017), the disturbed flow field for a solid translating in a stream with a uniform velocity gradient is dependent on the stream field and the relative translating velocity of the solid, i.e.

$$\mathbf{v}_w = \mathbf{v}_s + \mathbf{v} \tag{4}$$

where $\mathbf{v}_w$ is the flow field induced by a solid translating in the stream with velocity $\mathbf{v}_D$. $\mathbf{v}$ is the flow field induced by a solid translating in non-stream circumstance with velocity $\mathbf{v}_D-\mathbf{v}_s(\mathbf{r}_D)$, i.e. the relative velocity $\mathbf{v}_{Dr}$ in the stream field. According to the linear relationship between the induced flow field and the translating velocity of the solid, Eq. (4) can be further clarified as

$$\begin{aligned}\mathbf{v}_w = \mathbf{v}_s &+ [\mathbf{v}_D-\mathbf{v}_s(\mathbf{r}_D)]\cdot\mathbf{i}\mathbf{v}_1 \\ &+[\mathbf{v}_D-\mathbf{v}_s(\mathbf{r}_D)]\cdot\mathbf{j}\mathbf{v}_2+[\mathbf{v}_D-\mathbf{v}_s(\mathbf{r}_D)]\cdot\mathbf{k}\mathbf{v}_3\end{aligned} \tag{5}$$

where $\mathbf{v}_1,\mathbf{v}_2,\mathbf{v}_3$ is the induced flow field in the non-stream circumstance when the translating velocity is $\mathbf{v}_D = \mathbf{i},\mathbf{j},\mathbf{k}$ respectively. Let $\mathbf{v}_v = \mathbf{i}\mathbf{v}_1+\mathbf{j}\mathbf{v}_2+\mathbf{k}\mathbf{v}_3$ and $\mathbf{v}_{Dr}(\mathbf{r}_D) = \mathbf{v}_D-\mathbf{v}_s(\mathbf{r}_D)$, Eq. (5) can be simplified as

$$\mathbf{v}_w = \mathbf{v}_s + \mathbf{v}_{Dr}(\mathbf{r}_D)\cdot\mathbf{v}_v \tag{6}$$

2.2. Added masses and their computation method

The study later would show that the hydrodynamic force formula is dependent on the added masses of the solid. Traditionally, the added mass is expressed as a function of the flow field velocity-potential (Batchelor, 1967; Carbone et al., 2019). In this subsection, a new and convenient velocity-vector based computation method for the classical added mass would be introduced. Then, the concept of a generalized added mass, its computation method as well as its characters would be introduced and analyzed.

2.2.1. Computation method for the classical added mass

In inviscid flow, the velocity-potential based hydrodynamic force formula, which is also copied as Eq. (74) in Section 4.2, had been proposed by Newman (2017). Utilizing the DMT formula (86) in the

appendix, the following velocity-vector based hydrodynamic force formula can be obtained

$$\begin{aligned}\mathbf{F}_w = &-\frac{\rho}{N-1}\frac{\mathrm{d}}{\mathrm{d}t}\int_{S_i}\mathbf{r}_w\times(\mathbf{v}_w\times\mathbf{n})\mathrm{d}S\\ &-\int_{S_e}\rho\mathbf{v}_w\mathbf{v}_w\cdot\mathbf{n}\mathrm{d}S+\rho\int_{S_e}\mathbf{n}(v_w^2/2)\mathrm{d}S\end{aligned} \tag{7}$$

For the non-stream circumstance $\mathbf{v}_w=\mathbf{v}$ and $\mathbf{v}\to 0$ when the position of S_e tends to infinity. Consequently, the integration on S_e tends to zero and the hydrodynamic force in non-stream circumstance is

$$\begin{aligned}\mathbf{F} = &-\frac{\mathrm{d}\mathbf{v}_D}{\mathrm{d}t}\cdot\mathbf{i}\frac{\rho}{N-1}\int_{S_i}\mathbf{r}\times(\mathbf{v}_1\times\mathbf{n})\mathrm{d}S\\ &-\frac{\mathrm{d}\mathbf{v}_D}{\mathrm{d}t}\cdot\mathbf{j}\frac{\rho}{N-1}\frac{\mathrm{d}}{\mathrm{d}t}\int_{S_i}\mathbf{r}\times(\mathbf{v}_2\times\mathbf{n})\mathrm{d}S\\ &-\frac{\mathrm{d}\mathbf{v}_D}{\mathrm{d}t}\cdot\mathbf{k}\frac{\rho}{N-1}\frac{\mathrm{d}}{\mathrm{d}t}\int_{S_i}\mathbf{r}\times(\mathbf{v}_3\times\mathbf{n})\mathrm{d}S\end{aligned} \tag{8}$$

According to the concept of the classical added mass,

$$\mathbf{F}=-\mathbf{M}_{FV}\cdot\frac{\mathrm{d}\mathbf{v}_D}{\mathrm{d}t}=-\frac{\mathrm{d}\mathbf{v}_D}{\mathrm{d}t}\cdot\mathbf{M}_{FV} \tag{9}$$

$\mathbf{M}_{FV}$ is the added mass tensor accounting for the effect of translating acceleration on the hydrodynamic force. The corresponding matrix of $\mathbf{M}_{FV}$ is symmetric with the following elements

$$\mathbf{M}_{FV}=\begin{bmatrix}m_{11} & m_{12} & m_{13}\\ m_{12} & m_{22} & m_{23}\\ m_{13} & m_{23} & m_{33}\end{bmatrix} \tag{10}$$

By comparison between (8) and (9), one gets

$$m_{\epsilon\sigma}=\boldsymbol{\epsilon}\cdot\frac{\rho}{N-1}\int_{S_i}\mathbf{r}\times(\mathbf{v}_\sigma\times\mathbf{n})\mathrm{d}S \tag{11}$$

where $\epsilon=i,j,k;\sigma=1,2,3$. The equation above is a velocity-vector based expression for the classical added mass. It can be used to compute the added mass as the $\mathbf{v}_\sigma,\sigma=1.2.3$ can be determined by the panel method (Hess and Smith, 1967; Katz and Plotkin, 2001).

2.2.2. The generalized added mass and its computation method

For a rigid body with a given form, its generalized added mass in the Ox, Oy, Oz direction respectively is defined as

$$\xi_1=\rho\int_{R_b'-R_b}\mathbf{r}\boldsymbol{\omega}_1\mathrm{d}V,\quad \xi_2=\rho\int_{R_b'-R_b}\mathbf{r}\boldsymbol{\omega}_2\mathrm{d}V,\quad \xi_3=\rho\int_{R_b'-R_b}\mathbf{r}\boldsymbol{\omega}_3\mathrm{d}V \tag{12}$$

$\boldsymbol{\omega}_1,\boldsymbol{\omega}_2,\boldsymbol{\omega}_3$ is the vorticity distribution between the slip boundary layer $R_b'-R_b$ when the solid translates with velocity $\mathbf{i},\mathbf{j},\mathbf{k}$ respectively. To compute these added mass based on the panel method, the expression above should also be transformed to be velocity-vector based. According to the algebraic identity (91),

$$\begin{cases}\nabla\times(x\mathbf{v}_1)=\nabla x\times\mathbf{v}_1+x\nabla\times\mathbf{v}_1=\mathbf{i}\times\mathbf{v}_1+x\boldsymbol{\omega}_1\\ \nabla\times(y\mathbf{v}_1)=\nabla y\times\mathbf{v}_1+y\nabla\times\mathbf{v}_1=\mathbf{j}\times\mathbf{v}_1+y\boldsymbol{\omega}_1\\ \nabla\times(z\mathbf{v}_1)=\nabla z\times\mathbf{v}_1+z\nabla\times\mathbf{v}_1=\mathbf{k}\times\mathbf{v}_1+z\boldsymbol{\omega}_1\end{cases} \tag{13}$$

Left multiplying these identities with $\mathbf{i},\mathbf{j},\mathbf{k}$ respectively and then sum them up, one gets

$$\mathbf{i}\nabla\times(x\mathbf{v}_1)+\mathbf{j}\nabla\times(y\mathbf{v}_1)+\mathbf{k}\nabla\times(z\mathbf{v}_1)=(\mathbf{ii}+\mathbf{jj}+\mathbf{kk})\times\mathbf{v}_1+\mathbf{r}\boldsymbol{\omega}_1 \tag{14}$$

Noticing that the volume in $R_b'-R_b$ is almost zero and the value of $\mathbf{v}_1$ is limited, $\int_{R_b'-R_b}\mathbf{v}_1\mathrm{d}V=0$ or

$$\int_{R_b'-R_b}v_{1,x}\mathrm{d}R=\int_{R_b'-R_b}v_{1,y}\mathrm{d}R=\int_{R_b'-R_b}v_{1,z}\mathrm{d}R=0 \tag{15}$$

Substituting the two Eqs. (14) and (15) into Eq. (12) and then use the Gauss formula, one gets

$$\begin{aligned}\xi_1/\rho=&\mathbf{i}\int_{S_b}[\mathbf{n}\times(x\mathbf{v}_1)]\mathrm{d}S+\mathbf{j}\int_{S_b}[\mathbf{n}\times(y\mathbf{v}_1)]\mathrm{d}S\\ &+\mathbf{k}\int_{S_b}[\mathbf{n}\times(z\mathbf{v}_1)]\mathrm{d}S-\mathbf{i}\int_{S_i}[\mathbf{n}\times(x\mathbf{v}_1)]\mathrm{d}S\\ &-\mathbf{j}\int_{S_i}[\mathbf{n}\times(y\mathbf{v}_1)]\mathrm{d}S-\mathbf{k}\int_{S_i}[\mathbf{n}\times(z\mathbf{v}_1)]\mathrm{d}S\\ =&\int_{S_b}\mathbf{r}(\mathbf{n}\times\mathbf{v}_1)\mathrm{d}S-\int_{S_i}\mathbf{r}(\mathbf{n}\times\mathbf{v}_1)\mathrm{d}S\end{aligned} \tag{16}$$

As the velocity on S_b is given, the velocity distribution on S_i can be determined by the panel method, the equation above can be used to compute the generalized added mass ξ_1. ξ_1 is dependent on not only the shape but also the volume of the solid. For the same shaped solids, $\mathbf{r}$ and $\mathrm{d}S$ will increase k and k^2 times respectively when the scale of the solid increases k times. Consequently, all the elements in ξ_1 will increase k^3 times respectively, i.e., they are proportional with the volume of the solid. This would be helpful in tabulating the elements of ξ_1. Comparison between Eqs. (11) and (16) shows that the unit of the elements in ξ_1 is also same to mass. Consequently, ξ_1 is called the generalized added mass so that its relationship with the classical added mass can be clarified and distinguished.

Similarly, the generalized added mass ξ_2 and ξ_3 can be evaluated with the following formulas

$$\begin{cases}\xi_2/\rho=\displaystyle\int_{S_b}\mathbf{r}(\mathbf{n}\times\mathbf{v}_2)\mathrm{d}S-\int_{S_i}\mathbf{r}(\mathbf{n}\times\mathbf{v}_2)\mathrm{d}S\\ \xi_3/\rho=\displaystyle\int_{S_b}\mathbf{r}(\mathbf{n}\times\mathbf{v}_3)\mathrm{d}S-\int_{S_i}\mathbf{r}(\mathbf{n}\times\mathbf{v}_3)\mathrm{d}S\end{cases} \tag{17}$$

2.2.3. The characteristic of ξ_1,ξ_2,ξ_3 in three dimensional flow

In three dimensional flow, ξ_1,ξ_2,ξ_3 are all second-order tensor and there are 9 elements in their matrixes respectively. This is not convenient for tabulating the value of these elements. It will be shown in this subsection that ξ_1,ξ_2,ξ_3 are all antisymmetric matrixes and there is only six non-zero independent elements in these matrixes respectively, i.e.

$$\xi_1+\xi_1^{\mathrm{T}}=0,\quad \xi_2+\xi_2^{\mathrm{T}}=0,\quad \xi_3+\xi_3^{\mathrm{T}}=0 \tag{18}$$

The matrix form of Eq. (16) is

$$\xi_1=\int_{S_b}\mathbf{r}^{\mathrm{T}}\tilde{\mathbf{n}}\mathbf{v}_1\mathrm{d}S-\int_{S_i}\mathbf{r}^{\mathrm{T}}\tilde{\mathbf{n}}\mathbf{v}_1\mathrm{d}S \tag{19}$$

where $\tilde{\mathbf{a}}$ is the skew-symmetric matrix of $\mathbf{a}=a_1\mathbf{i}+a_2\mathbf{j}+a_3\mathbf{k}$, i.e.

$$\tilde{\mathbf{a}}=\begin{bmatrix}0 & -a_3 & a_2\\ a_3 & 0 & -a_1\\ -a_2 & a_1 & 0\end{bmatrix} \tag{20}$$

According to the antisymmetry of $\tilde{\mathbf{a}}$, it is not difficult to show

$$\xi_1^{\mathrm{T}}=-\int_{S_b}\mathbf{v}_1^{\mathrm{T}}\tilde{\mathbf{n}}\mathbf{r}\mathrm{d}S+\int_{S_i}\mathbf{v}_1^{\mathrm{T}}\tilde{\mathbf{n}}\mathbf{r}\mathrm{d}S \tag{21}$$

Consequently

$$\begin{aligned}\xi_1+\xi_1^{\mathrm{T}}=&\int_{S_b}(-\mathbf{r}^{\mathrm{T}}\tilde{\mathbf{v}}_1+\mathbf{v}_1^{\mathrm{T}}\tilde{\mathbf{r}})\mathbf{n}\mathrm{d}S-\int_{S_i}(-\mathbf{r}^{\mathrm{T}}\tilde{\mathbf{v}}_1+\mathbf{v}_1^{\mathrm{T}}\tilde{\mathbf{r}})\mathbf{n}\mathrm{d}S\\ =&2\int_{S_b}(\tilde{\mathbf{v}}_1\mathbf{r})^{\mathrm{T}}\mathbf{n}\mathrm{d}S-2\int_{S_i}(\tilde{\mathbf{v}}_1\mathbf{r})^{\mathrm{T}}\mathbf{n}\mathrm{d}S\end{aligned} \tag{22}$$

Transform the equation above and rewritten the equation above in vector form, one gets

$$\begin{aligned}\xi_1+\xi_1^{\mathrm{T}}=&2\int_{S_b}\mathbf{n}(\mathbf{v}_1\times\mathbf{r})\mathrm{d}S-2\int_{S_i}\mathbf{n}(\mathbf{v}_1\times\mathbf{r})\mathrm{d}S\\ =&2\int_{R_b'-R_b}\nabla(\mathbf{v}_1\times\mathbf{r})\mathrm{d}R=-2\int_{R_b'-R_b}\tilde{\mathbf{v}}_1\mathrm{d}R\end{aligned} \tag{23}$$

where ξ_1^{T} represent the second order tensor corresponding to matrix ξ_1^{T}(As mentioned in Section 2.1.1, the notation of a tensor ξ_1^{T} appears

the same to its corresponding matrix ξ_1^{T} due to the font design of the journal. This phenomenon also happens on tensor $\tilde{\mathbf{v}}_1$). $\tilde{\mathbf{v}}_1$ is the tensor corresponding to matrix $\tilde{\mathbf{v}}_1$. The Gauss formula is applied in the second equal of the equation above. The matrix form of the equation above is

$$\xi_1 + \xi_1^{\mathrm{T}} = 2\int_{R_b'-R_b}\begin{bmatrix} 0 & v_{1,z} & -v_{1,y} \\ -v_{1,z} & 0 & v_{1,x} \\ v_{1,y} & -v_{1,x} & 0 \end{bmatrix}\mathrm{d}R \tag{24}$$

Considering Eq. (15), one gets $\xi_1 + \xi_1^{\mathrm{T}} = 0$. This result shows that ξ_1 is an antisymmetric matrix and only six independent elements in it is non-zero.

It can be similarity shown that $\xi_2 + \xi_2^{\mathrm{T}} = 0$ and $\xi_3 + \xi_3^{\mathrm{T}} = 0$, i.e. Eq. (18) is true.

2.3. Hydrodynamic force in the uniform velocity gradient stream

2.3.1. Decomposition of the hydrodynamic force

Substituting the velocity distribution formula (6) into the hydrodynamic force formula (7), one gets

$$\begin{aligned}\mathbf{F}_w = &-\frac{\rho}{N-1}\frac{\mathrm{d}}{\mathrm{d}t}\int_{S_i}\mathbf{r}\times[(\mathbf{v}_s+\mathbf{v}_{Dr}\cdot\mathbf{v}_v)\times\mathbf{n}]\mathrm{d}S \\ &-\rho\int_{S_e}(\mathbf{v}_s+\mathbf{v}_{Dr}\cdot\mathbf{v}_v)(\mathbf{v}_s+\mathbf{v}_{Dr}\cdot\mathbf{v}_v)\cdot\mathbf{n}\mathrm{d}S \\ &+\frac{\rho}{2}\int_{S_e}\mathbf{n}(\mathbf{v}_s+\mathbf{v}_{Dr}\cdot\mathbf{v}_v)\cdot(\mathbf{v}_s+\mathbf{v}_{Dr}\cdot\mathbf{v}_v)\mathrm{d}S\end{aligned} \tag{25}$$

The $\mathbf{r}_w$ has been changed to $\mathbf{r}$ in the equation above. The rationality of this treatment is obvious as the hydrodynamic force should not be dependent on the starting point of the flow field position vector. Expand the binomial in the equation above, one gets

$$\mathbf{F} = \mathbf{F}_{ss} + \mathbf{F}_{XX} + \mathbf{F}_{sX} + \mathbf{F}_{XY} \tag{26}$$

where $\mathbf{F}_{ss}$ represents the terms that include $\mathbf{v}_s$ only in $\mathbf{F}$, $\mathbf{F}_{XX}$ represents the terms that include $\mathbf{v}_i, i = 1 \sim 3$ only in $\mathbf{F}$, $\mathbf{F}_{sX}$ represents the terms that include the cross multiplication of $\mathbf{v}_s$ and $\mathbf{v}_m, m = 1 \sim 3$ only in $\mathbf{F}$, $\mathbf{F}_{XY}$ represents the terms that include the cross multiplication of $\mathbf{v}_n, n = 1 \sim 3$ and $\mathbf{v}_m, m = 1 \sim 3, m \neq n$ in only $\mathbf{F}$. The exact expression of $\mathbf{F}_{ss}, \mathbf{F}_{XX}, \mathbf{F}_{sX}, \mathbf{F}_{XY}$ are list as follow respectively

$$\begin{cases}\mathbf{F}_{ss} = -\dfrac{\mathrm{d}}{\mathrm{d}t}\mathbf{A}_1 - \mathbf{A}_2, \quad \mathbf{A}_1 = \dfrac{\rho}{N-1}\displaystyle\int_{S_i}\mathbf{r}\times(\mathbf{v}_s\times\mathbf{n})\mathrm{d}S \\ \mathbf{A}_2 = \displaystyle\int_{S_e}\rho\mathbf{v}_s\mathbf{v}_s\cdot\mathbf{n}\mathrm{d}S - \frac{\rho}{2}\int_{S_e}\mathbf{n}\mathbf{v}_s\cdot\mathbf{v}_s\mathrm{d}S\end{cases} \tag{27}$$

$$\begin{cases}\mathbf{F}_{XX} = \displaystyle\sum_{m=1\sim3}\mathbf{F}_m, \quad \mathbf{F}_m = -\frac{\mathrm{d}}{\mathrm{d}t}\left(v_{Dr,m}\mathbf{B}_m\right) - \rho v_{Dr,m}^2 * \mathbf{C}_m \\ \mathbf{B}_m = \dfrac{\rho}{N-1}\displaystyle\int_{S_i}\mathbf{r}\times(\mathbf{v}_m\times\mathbf{n})\mathrm{d}S \\ \mathbf{C}_m = \displaystyle\int_{S_e}\mathbf{v}_m\mathbf{v}_m\cdot\mathbf{n}\mathrm{d}S - \frac{1}{2}\int_{S_e}\mathbf{n}\mathbf{v}_m\cdot\mathbf{v}_m\mathrm{d}S\end{cases} \tag{28}$$

$$\begin{cases}\mathbf{F}_{sX} = \displaystyle\sum_{m=1\sim3}\mathbf{F}_{sm}, \quad \mathbf{F}_{sm} = -\rho v_{Dr,m} * \mathbf{D}_m \\ \mathbf{D}_m = \displaystyle\int_{S_e}(\mathbf{v}_s\mathbf{v}_m + \mathbf{v}_m\mathbf{v}_s)\cdot\mathbf{n}\mathrm{d}S - \int_{S_e}\mathbf{n}\mathbf{v}_s\cdot\mathbf{v}_m\mathrm{d}S\end{cases} \tag{29}$$

$$\begin{cases}\mathbf{F}_{XY} = \displaystyle\sum_{n=1\sim3}\left(\sum_{m=1\sim3,m\neq n}\mathbf{F}_{mn}\right), \quad \mathbf{F}_{mn} = -\rho v_{Dr,m}v_{Dr,n} * \mathbf{E}_{mn} \\ \mathbf{E}_{mn} = \displaystyle\int_{S_e}\mathbf{v}_m\mathbf{v}_n\cdot\mathbf{n}\mathrm{d}S - \frac{1}{2}\int_{S_e}\mathbf{n}\mathbf{v}_m\cdot\mathbf{v}_n\mathrm{d}S\end{cases} \tag{30}$$

where $v_{Dr,m}, v_{Dr,n}; m, n = 1, 2, 3$ is the three components of $\mathbf{v}_{Dr}$ respectively.

2.3.2. Simplification of $\mathbf{F}_{ss}$

As $\mathbf{v}_s$ is continuous and derivable in R_b', the DMT formula (87) is applicable on it. Further noticing that $\nabla\times\mathbf{v}_s = 0$ on R_b' and $\mathbf{n}$ is pointing inside R_b' on S_i, the $\mathbf{A}_1$ in Eq. (27) can be rewritten as

$$\mathbf{A}_1 = -\rho\int_{R_b'}\mathbf{v}_s\mathrm{d}V = -\rho\int_{R_b'}[\mathbf{v}_s(\mathbf{r}_D) + (\mathbf{r}-\mathbf{r}_D)\cdot\boldsymbol{\Phi}]\mathrm{d}V \tag{31}$$

According to the definition of the volume center $\mathbf{r}_V$, one knows that $\mathbf{r}_V V_b = \int_{R_b'}\mathbf{r}\mathrm{d}V$ where V_b is the volume of R_b'. Thus

$$\mathbf{A}_1 = -\rho V_b[\mathbf{v}_s(\mathbf{r}_D) + (\mathbf{r}_V - \mathbf{r}_D)\cdot\boldsymbol{\Phi}] = -\bar{m}\mathbf{v}_s(\mathbf{r}_V) \tag{32}$$

where $\bar{m} = \rho V_b$ is the mass of the fluid displaced by the solid.

By applying the Gauss formula, the $\mathbf{A}_2$ in Eq. (27) can be rewritten as

$$\begin{aligned}\mathbf{A}_2 &= \rho\int_{R_f\cup R_b'}\nabla\cdot(\mathbf{v}_s\mathbf{v}_s)\mathrm{d}V - \frac{\rho}{2}\int_{R_f\cup R_b'}\nabla(\mathbf{v}_s\cdot\mathbf{v}_s)\mathrm{d}V \\ &= \frac{\rho}{2}\int_{R_f\cup R_b'}[2\nabla\cdot(\mathbf{v}_s\mathbf{v}_s) - \nabla(\mathbf{v}_s\cdot\mathbf{v}_s)]\mathrm{d}V\end{aligned} \tag{33}$$

It is not difficult to show that $2\nabla\cdot(\mathbf{v}_s\mathbf{v}_s) = \nabla(\mathbf{v}_s\cdot\mathbf{v}_s)$ by applying the identity (90) and (92), consequently $\mathbf{A}_2 = 0$.

Substituting the simplified expression of $\mathbf{A}_1, \mathbf{A}_2$ into the formula (27), the $\mathbf{F}_{ss}$ can be simplified as

$$\begin{aligned}\mathbf{F}_{ss} &= \bar{m}\frac{\mathrm{d}\mathbf{v}_s(\mathbf{r}_V)}{\mathrm{d}t} = \bar{m}\lim_{\Delta t\to0}\frac{1}{\Delta t}[\mathbf{v}_s(\mathbf{r}_V + \mathbf{v}_D\Delta t) - \mathbf{v}_s(\mathbf{r}_V)] \\ &= \bar{m}\lim_{\Delta t\to0}\frac{\mathbf{v}_D\Delta t\cdot\boldsymbol{\Phi}}{\Delta t} = \bar{m}\mathbf{v}_D\cdot\boldsymbol{\Phi}\end{aligned} \tag{34}$$

For a solid resting in the stream $\mathbf{v}_D = 0$. Consequently, $\mathbf{F}_{ss} = 0$ according to the equation above. This is obvious as $\mathbf{F}_{ss}$ represents the hydrodynamic force due to the unsteady motion of the fluid.

2.3.3. Simplification of $\mathbf{F}_{XX}$ and $\mathbf{F}_{XY}$

When the solid translates with unit velocity $\mathbf{v} = \mathbf{m}, m = 1, 2, 3$, the $\mathbf{B}_m$ in Eq. (28) can be evaluated by the following formulas according to Eq. (11)

$$\begin{cases}\mathbf{B}_1 = \dfrac{\rho}{N-1}\displaystyle\int_{S_i}\mathbf{r}\times(\mathbf{v}_1\times\mathbf{n})\mathrm{d}S = m_{11}\mathbf{i} + m_{12}\mathbf{j} + m_{13}\mathbf{k} \\ \mathbf{B}_2 = \dfrac{\rho}{N-1}\displaystyle\int_{S_i}\mathbf{r}\times(\mathbf{v}_2\times\mathbf{n})\mathrm{d}S = m_{12}\mathbf{i} + m_{22}\mathbf{j} + m_{23}\mathbf{k} \\ \mathbf{B}_3 = \dfrac{\rho}{N-1}\displaystyle\int_{S_i}\mathbf{r}\times(\mathbf{v}_3\times\mathbf{n})\mathrm{d}S = m_{13}\mathbf{i} + m_{23}\mathbf{j} + m_{33}\mathbf{k}\end{cases} \tag{35}$$

The expression of $\mathbf{C}_1$ in this case is

$$\mathbf{C}_1 = \int_{S_e}\mathbf{v}_1\mathbf{v}_1\cdot\mathbf{n}\mathrm{d}S - \frac{1}{2}\int_{S_e}\mathbf{n}\mathbf{v}_1\cdot\mathbf{v}_1\mathrm{d}S \tag{36}$$

Noticing that $\mathbf{v}_1$ would decrease exponentially with the increase of the distance between S_e and S_b (Wu et al., 2015), $\mathbf{A}_1$ or $\mathbf{B}_m, m = 1, 2, 3$ reduce to zero when S_e is far enough from S_b. For the same reason, $\mathbf{C}_1 = 0$ as $\mathbf{C}_1$ is independent on the position of S_e. Similarly, $\mathbf{C}_m = 0, m = 2, 3$; $\mathbf{E}_{mn} = 0, m, n = 1, 2, 3, m \neq n$. Substituting these results into Eqs. (28) and (30), $\mathbf{F}_{XX}$ and $\mathbf{F}_{XY}$ can be simplified as follow respectively

$$\mathbf{F}_{XX} = -\frac{\mathrm{d}\mathbf{v}_{Dr}}{\mathrm{d}t}\cdot\mathbf{M}_{FV} \tag{37}$$

$$\mathbf{F}_{XY} = \sum_{n=1}^{3}\left(\sum_{m=1,m\neq n}^{3}\mathbf{F}_{mn}\right) = 0 \tag{38}$$

2.3.4. The first simplification method for F_{sX}

$\mathbf{v}_s$ is continuous and derivable on $R_f'\cup R_b'$. However, $\mathbf{v}_1$ is continuous and derivable on R_f' only. Take a sub-region R_{b1}' in R_b'. Let the velocity distribution $\mathbf{v}_1$ on R_{b1}' be the uniform distribution $\mathbf{i}$. The distribution of $\mathbf{v}_1$ on $R_b' - R_{b1}'$ is so adjusted so that it is continuous and derivable on $R_b'\cup R_f'$. When R_{b1}' is increased to the case that $R_{b1}' = R_b$, the

distribution of $\mathbf{v}_1$ on R_b' is exactly the uniform velocity $\mathbf{i}$ on R_b and the vorticity layer on $R_b' - R_b'$. As $\mathbf{v}_1$ is now also continuous and derivable on $R_f' \cup R_b'$, the Gauss formula can be applied. By applying the identity (90) and (92), one gets

$$\begin{aligned}&\nabla\cdot(\mathbf{v}_s\mathbf{v}_1)+\nabla\cdot(\mathbf{v}_1\mathbf{v}_s)-\nabla(\mathbf{v}_s\cdot\mathbf{v}_1)=(\nabla\cdot\mathbf{v}_1)\mathbf{v}_s\\&+(\nabla\cdot\mathbf{v}_s)\mathbf{v}_1-\mathbf{v}_1\times(\nabla\times\mathbf{v}_s)-\mathbf{v}_s\times(\nabla\times\mathbf{v}_1)\end{aligned}\tag{39}$$

Noticing that $\nabla\times\mathbf{v}_s=0, \nabla\cdot\mathbf{v}_1=0, \nabla\cdot\mathbf{v}_s=0$ on $R_b\cup R_f$ and $\nabla\times\mathbf{v}_1$ is non-zero on $R_b'-R_b$ only, the $\mathbf{D}_1$ in Eq. (29) can be rewritten as follow

$$-\mathbf{D}_1=\int_{R_b'-R_b}\mathbf{v}_s\times\boldsymbol{\omega}_1\mathrm{d}V\tag{40}$$

Considering Eq. (1) and the vorticity conservation theorem $\int_{R_b'-R_b}\boldsymbol{\omega}_1\mathrm{d}V=0$, the right part of the equation above can be rewritten as

$$\begin{aligned}&\int_{R_b'-R_b}\mathbf{v}_s\times\boldsymbol{\omega}_1\mathrm{d}V=\int_{R_b'-R_b}[\mathbf{v}_s(\mathbf{r}_D)+(\mathbf{r}-\mathbf{r}_D)\cdot\boldsymbol{\Phi}]\times\boldsymbol{\omega}_1\mathrm{d}V\\&=\int_{R_b'-R_b}\mathbf{r}\cdot\boldsymbol{\Phi}\times\boldsymbol{\omega}_1\mathrm{d}V\end{aligned}\tag{41}$$

Utilizing Eq. (3), one gets $\mathbf{r}\cdot\boldsymbol{\Phi}\times\boldsymbol{\omega}_1=-\mathbf{i}\cdot\mathbf{r}\omega_1\times\boldsymbol{\phi}_x-\mathbf{j}\cdot\mathbf{r}\omega_1\times\boldsymbol{\phi}_y-\mathbf{k}\cdot\mathbf{r}\omega_1\times\boldsymbol{\phi}_z$. Substituting this result into Eq. (41) and considering the definition of the generalized added mass (12), one gets

$$\mathbf{D}_1=-\int_{R_b'-R_b}\mathbf{v}_s\times\boldsymbol{\omega}_1\mathrm{d}V=-\boldsymbol{\phi}_x\times\boldsymbol{\xi}_{1,x}-\boldsymbol{\phi}_y\times\boldsymbol{\xi}_{1,y}-\boldsymbol{\phi}_z\times\boldsymbol{\xi}_{1,z}\tag{42}$$

Similarly, the $\mathbf{D}_2, \mathbf{D}_3$ can be simplified as

$$\begin{cases}\mathbf{D}_2=-\boldsymbol{\phi}_x\times\boldsymbol{\xi}_{2,x}-\boldsymbol{\phi}_y\times\boldsymbol{\xi}_{2,y}-\boldsymbol{\phi}_z\times\boldsymbol{\xi}_{2,z}\\\mathbf{D}_3=-\boldsymbol{\phi}_x\times\boldsymbol{\xi}_{3,x}-\boldsymbol{\phi}_y\times\boldsymbol{\xi}_{3,y}-\boldsymbol{\phi}_z\times\boldsymbol{\xi}_{3,z}\end{cases}\tag{43}$$

Substituting the expression of $\mathbf{D}_1, \mathbf{D}_2, \mathbf{D}_3$ into Eq. (29), one gets the simplified expression of $\mathbf{F}_{sX}$ after some algebra operation

$$\mathbf{F}_{sX}=\sum_{m=1\sim3}\mathbf{F}_{sm}=\rho[\boldsymbol{\phi}_x\times(\mathbf{v}_{Dr}\cdot\boldsymbol{\Xi}_x)+\boldsymbol{\phi}_y\times(\mathbf{v}_{Dr}\cdot\boldsymbol{\Xi}_y)+\boldsymbol{\phi}_z\times(\mathbf{v}_{Dr}\cdot\boldsymbol{\Xi}_z)]\tag{44}$$

where

$$\begin{cases}\boldsymbol{\Xi}_x=\mathbf{i}\xi_{1,x}+\mathbf{j}\xi_{2,x}+\mathbf{k}\xi_{3,x}\\\boldsymbol{\Xi}_y=\mathbf{j}\xi_{1,y}+\mathbf{j}\xi_{2,y}+\mathbf{k}\xi_{3,y}\\\boldsymbol{\Xi}_z=\mathbf{k}\xi_{1,z}+\mathbf{j}\xi_{2,z}+\mathbf{k}\xi_{3,z}\end{cases}\tag{45}$$

2.3.5. The second simplification method for F_{sX}

For incompressible flow, it can be shown that

$$\int_{R_b'-R_b}\mathbf{r}\cdot\boldsymbol{\Phi}\times\boldsymbol{\omega}_1\mathrm{d}V=-\frac{1}{N-1}\int_{R_b'-R_b}\boldsymbol{\Phi}\cdot(\mathbf{r}\times\boldsymbol{\omega}_1)\mathrm{d}V\tag{46}$$

where N is the dimension of the flow field. The detailed proof of the equation above can be referred to the appendix. According to this formula, Eq. (41) can be rewritten as

$$\begin{aligned}&\int_{R_b'-R_b}\mathbf{v}_s\times\boldsymbol{\omega}_1\mathrm{d}V=-\frac{1}{N-1}\boldsymbol{\Phi}\cdot\int_{R_b'-R_b}(\mathbf{r}\times\boldsymbol{\omega}_1)\mathrm{d}V\\&=-\frac{\boldsymbol{\Phi}}{N-1}\cdot\left[-\int_{S_b}\mathbf{r}\times(\mathbf{i}\times\mathbf{n})\mathrm{d}S+\int_{S_i}\mathbf{r}\times(\mathbf{v}\times\mathbf{n})\mathrm{d}S\right]\end{aligned}\tag{47}$$

The last equal in the equation above is due to DMT formula (87), the different sign before the integration on S_i and S_b is due to the definition of the positive $\mathbf{n}$ on these two surfaces. By applying the DMT formula (87) again, one gets

$$-\frac{1}{N-1}\int_{S_b}\mathbf{r}\times(\mathbf{i}\times\mathbf{n})\mathrm{d}S=\int_{R_b}\mathbf{i}dR=V_b\mathbf{i}\tag{48}$$

According to the relationship between the flow field momentum and the added mass shown in Eq. (35) and noticing the positive direction of $\mathbf{n}$ on S_i, one gets

$$\frac{1}{N-1}\int_{S_i}\mathbf{r}\times(\mathbf{v}_1\times\mathbf{n})\mathrm{d}S=\frac{1}{\rho}(m_{11}\mathbf{i}+m_{12}\mathbf{j}+m_{13}\mathbf{k})\tag{49}$$

Combining the three equations above one gets the expression of $\int_{R_b'-R_b}\mathbf{v}_s\times\boldsymbol{\omega}_1\mathrm{d}V$. Substituting this result into Eq. (40), one gets

$$\mathbf{D}_1=\boldsymbol{\Phi}\cdot(\bar{m}\mathbf{i}+m_{11}\mathbf{i}+m_{12}\mathbf{j}+m_{13}\mathbf{k})\tag{50}$$

Similarly

$$\begin{cases}\mathbf{D}_2=\boldsymbol{\Phi}\cdot(\bar{m}\mathbf{j}+m_{12}\mathbf{i}+m_{22}\mathbf{j}+m_{23}\mathbf{k})\\\mathbf{D}_3=\boldsymbol{\Phi}\cdot(\bar{m}\mathbf{k}+m_{13}\mathbf{i}+m_{23}\mathbf{j}+m_{33}\mathbf{k})\end{cases}\tag{51}$$

Substitute the expression of $\mathbf{D}_1, \mathbf{D}_2, \mathbf{D}_3$ into Eq. (29), one gets the following expression for $\mathbf{F}_{sX}$ after some algebra operation

$$\begin{aligned}&\mathbf{F}_{sX}=-\bar{m}\mathbf{v}_{Dr}\cdot\boldsymbol{\Phi}-\upsilon_{Dr,x}\boldsymbol{\Phi}\cdot(m_{11}\mathbf{i}+m_{12}\mathbf{j}+m_{13}\mathbf{k})\\&-\upsilon_{Dr,y}\boldsymbol{\Phi}\cdot(m_{12}\mathbf{i}+m_{22}\mathbf{j}+m_{23}\mathbf{k})-\upsilon_{Dr,z}\boldsymbol{\Phi}\cdot(m_{13}\mathbf{i}+m_{23}\mathbf{j}+m_{33}\mathbf{k})\\&=-\bar{m}\mathbf{v}_{Dr}\cdot\boldsymbol{\Phi}-\boldsymbol{\Phi}\cdot(\mathbf{v}_{Dr}\cdot\mathbf{M}_{FV})=-\mathbf{v}_{Dr}\cdot(\bar{m}\mathbf{I}+\mathbf{M}_{FV})\cdot\boldsymbol{\Phi}\end{aligned}\tag{52}$$

2.3.6. The final expression for hydrodynamic force

Substitute the simplified expression of $\mathbf{F}_{ss}, \mathbf{F}_{XX}, \mathbf{F}_{XY}, \mathbf{F}_{sX}$, i.e. Eqs. (34), (37), (38) and (44) into Eq. (26), the expression of $\mathbf{F}$ can be finally simplified as

$$\begin{aligned}&\mathbf{F}=\bar{m}\mathbf{v}_D\cdot\boldsymbol{\Phi}-\frac{\mathrm{d}\mathbf{v}_{Dr}}{\mathrm{d}t}\cdot\mathbf{M}_{FV}\\&+\rho[\boldsymbol{\phi}_x\times(\mathbf{v}_{Dr}\cdot\boldsymbol{\Xi}_x)+\boldsymbol{\phi}_y\times(\mathbf{v}_{Dr}\cdot\boldsymbol{\Xi}_y)+\boldsymbol{\phi}_z\times(\mathbf{v}_{Dr}\cdot\boldsymbol{\Xi}_z)]\end{aligned}\tag{53}$$

Noticing that $\mathbf{v}_{Dr}=\mathbf{v}_D-\mathbf{v}_s(\mathbf{r}_D)$ and Eq. (34), equation $\mathbf{F}$ can be rewritten as

$$\begin{aligned}&\mathbf{F}=\mathbf{v}_D\cdot\boldsymbol{\Phi}\cdot(\bar{m}\mathbf{I}+\mathbf{M}_{FV})-\frac{\mathrm{d}\mathbf{v}_D}{\mathrm{d}t}\cdot\mathbf{M}_{FV}\\&+\rho[\boldsymbol{\phi}_x\times(\mathbf{v}_{Dr}\cdot\boldsymbol{\Xi}_x)+\boldsymbol{\phi}_y\times(\mathbf{v}_{Dr}\cdot\boldsymbol{\Xi}_y)+\boldsymbol{\phi}_z\times(\mathbf{v}_{Dr}\cdot\boldsymbol{\Xi}_z)]\end{aligned}\tag{54}$$

where $\mathbf{I}$ is the unit tensor. According to either of the equations above, if the velocity gradient of the stream $\boldsymbol{\Phi}$ is given, the hydrodynamic force acted on a given form solid translating in the stream can be evaluated by first calculating its classical added mass $\mathbf{M}_{FV}$ according to Eq. (11) and then the generalized added mass according to Eq. (16) and (45).

If $\mathbf{F}_{sX}$'s expression (52) is adopted, then Eqs. (53) and (54) change as follow respectively

$$\mathbf{F}=\bar{m}\mathbf{v}_D\cdot\boldsymbol{\Phi}-\frac{\mathrm{d}\mathbf{v}_{Dr}}{\mathrm{d}t}\cdot\mathbf{M}_{FV}-\mathbf{v}_{Dr}\cdot(\bar{m}\mathbf{I}+\mathbf{M}_{FV})\cdot\boldsymbol{\Phi}\tag{55}$$

$$\mathbf{F}=\mathbf{v}_D\cdot\boldsymbol{\Phi}\cdot(\bar{m}\mathbf{I}+\mathbf{M}_{FV})-\frac{\mathrm{d}\mathbf{v}_D}{\mathrm{d}t}\cdot\mathbf{M}_{FV}-\mathbf{v}_{Dr}\cdot(\bar{m}\mathbf{I}+\mathbf{M}_{FV})\cdot\boldsymbol{\Phi}\tag{56}$$

Some skills are important in the proof above though it mainly follows the road proved by Newman (2017). The first skill is to replace the original velocity-potential based hydrodynamic force formula (74) with the velocity-vector based formula (25). The second skill is to decompose the stream velocity gradient $\boldsymbol{\Phi}$ into three dyads according to Eq. (3). Consequently the constant $\boldsymbol{\Phi}$ can be moved out of the integral sign in the last term in Eq. (41) and the hydrodynamic force expression can be simplified. In the proof of Eqs. (55) and (56), the most important skill is to prove that equal (46) is true.

3. Verification of the hydrodynamic force formulas

To verify the correctness of the hydrodynamic force formula (53)–(56), numerical examples are designed and exhibited. Firstly, the rationality of the Newman hypothesis, i.e. the correctness of Eq. (4) and (5) is checked. Then, the correctness of Eq. (53)–(56) is verified when the solid is resting in two-dimensional flow and three-dimensional flow respectively. At last, the correctness of Eqs. (53)–(56) is verified when the solid is translating.

3.1. Verification of the Newman hypothesis

The Newman hypothesis, i.e. Eq. (4) or (5) shows that the disturbed flow field $\mathbf{v}_w$ by a solid moving in uniform velocity gradient stream can be decomposed into the undisturbed stream field $\mathbf{v}_s$ and the disturbed flow field by the solid moving in the non-stream field with

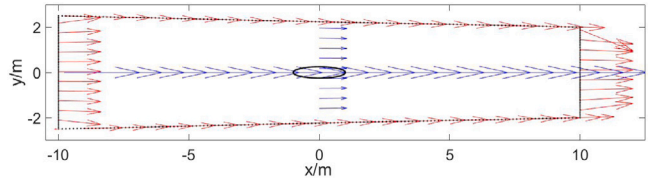

Fig. 2. The uniform velocity gradient flow field in an isosceles trapezoid.

velocity $\mathbf{v}_{Dr} = \mathbf{v}_D - \mathbf{v}_s$. To verify the correctness of this hypothesis, a two-dimensional stream field $\mathbf{v}_s$ with uniform velocity gradient is constructed in an isosceles trapezoid. The upper base is on the right side with a length 2 m. The lower base is on the left side with length 2.5 m. The height of the isosceles trapezoid is 20 m as shown in Fig. 2. When computing the undisturbed stream field with the panel method, the ellipse does not exist. The normal velocity on the right exit is set to uniform 1 m/s. The normal velocity on the left entrance is set to uniform 0.8 m/s according to the equation of continuity. The normal velocity on the upper and lower waist are both zero. The total panel on the boundary of the trapezoid is 200. The source strength on the panel is determined by the given normal velocity on the boundary. Then the velocity in the flow field is induced by these sources. To illustrate the stream velocity, a horizontal and a vertical line is drawn in the trapezoid passing through its center. The velocity-vector is plotted on these two lines as well as the boundary of the trapezoid. It can be seen from Fig. 2 that the velocity distribution is consistent with what is anticipated. Further analysis shows that the velocity gradient on the horizontal line is a little non-uniform. We change the two straight waste lines of the isosceles trapezoid with two curves so that the velocity gradient is uniform in the adjacent of the center. The upper waste is now a quartic curve determined by five points $(-10, 2.5), (-5, 2.37), (0, 2.2385), (5, 2.125)$ and $(10, 2)$. As the curves are almost coincident with the original waste of the isosceles trapezoid, the form of the new boundary is still called an isosceles trapezoid. The computation result show that the velocity gradient adjacent to the center is now $\phi_{11} = \partial v_x/\partial x = 0.0093/\mathrm{s}$, the pressure gradient is $\partial p/\partial x = -0.0079/\mathrm{s}$ and the velocity in the center is $v_{s,x} = 0.8524\,\mathrm{m/s}$.

Secondly, an ellipse with major axis $a = 1$ m and minor axis $b = 0.25$ m is put in the stream. The panel on the ellipse is 128 and the steam velocity $\mathbf{v}_s$ on it is computed based on the sources distributed on the isosceles trapezoid. Then, sources are distributed on the ellipse and the boundary normal velocity is set to zero. The strength of the sources on both the ellipse and the trapezoid is determined by applying the panel method again. At last, the induced flow field $\mathbf{v}_w$ is evaluated according to these sources. Thirdly, the induced velocity $\mathbf{v}$ when the solid is moving with velocity -0.8524 m/s in the non-stream field is computed by panel method. To check the rationality of the Newman hypothesis, the value of $(|\mathbf{v}_s + \mathbf{v}| - |\mathbf{v}_w|)/|\mathbf{v}_w| \times 100\%$ is calculated. The result shows that its maximum value is 3.02%, the minimum value is 0.42%, the average value is 2.67%. This indicates that $\mathbf{v}_w \approx \mathbf{v}_s + \mathbf{v}$ when $\boldsymbol{\Phi}$ is uniform and the Newman hypothesis (4) is verified.

3.2. Verification in two dimensional flow

This verification is divided into two parts. The first part checks the consistency of formula (53) or (54) and (55) or (56). The second part verifies the correctness of (53)–(56) with numerical results directly.

The two-dimensional problem can be regarded as a special case of three-dimensional flow in which the parameter in Oz direction is zero. Consequently, the matrix of velocity and velocity gradient can be written as

$$\upsilon_{Dr} = \begin{bmatrix} \upsilon_{Dr,x} \\ \upsilon_{Dr,y} \\ 0 \end{bmatrix}, \quad \boldsymbol{\Phi} = \begin{bmatrix} \phi_{11} & \phi_{12} & 0 \\ \phi_{21} & \phi_{22} & 0 \\ 0 & 0 & 0 \end{bmatrix} \tag{57}$$

Table 1
Numerical result of the added mass for ellipse under different slenderness ratio.

λ	1	2	3	4	5	6
m_{11}/kg	3.1415	0.7854	0.3491	0.1963	0.1257	0.0873
m_{22}/kg	3.1415	3.1415	3.1415	3.1415	3.1415	3.1415
$\bar{m}$/kg	3.1416	1.5708	1.0472	0.7854	0.6283	0.5236
$\xi_1(2,3)$/kg	6.2831	2.3562	1.3962	0.9817	0.7540	0.6109
$\xi_2(1,3)$/kg	−6.2831	−4.7123	−4.1887	−3.9269	−3.7699	−3.6652

According to Eqs. (45), (16) and (17), the tensor $\boldsymbol{\Xi}_x, \boldsymbol{\Xi}_y, \boldsymbol{\Xi}_z$ is dependent on tensor $\boldsymbol{\xi}_1, \boldsymbol{\xi}_2$ and $\boldsymbol{\xi}_3$ while the element of the latter is dependent on the velocity on body surface S_b and the slip boundary surface S_i. The velocity on S_b is identical to the translating velocity of the solid and the slip boundary velocity can be determined by panel method. For an ellipse, numerical result shows that only $\xi_1(1,3), \xi_1(2,3), \xi_2(1,3), \xi_2(2,3)$ are non-zero. Consequently, $\boldsymbol{\Xi}_z = 0$ and the matrix of tensor $\boldsymbol{\Xi}_x, \boldsymbol{\Xi}_y$ can be simplified as

$$\boldsymbol{\Xi}_x = \begin{bmatrix} 0 & 0 & \xi_1(1,3) \\ 0 & 0 & \xi_2(1,3) \\ 0 & 0 & 0 \end{bmatrix}, \quad \boldsymbol{\Xi}_y = \begin{bmatrix} 0 & 0 & \xi_1(2,3) \\ 0 & 0 & \xi_2(2,3) \\ 0 & 0 & 0 \end{bmatrix} \tag{58}$$

Substitute these results into the hydrodynamic force formulas (53) or (54), these two hydrodynamic force formulas for an ellipsoid resting in two-dimensional uniform gradient flow can be both simplified as

$$\begin{aligned} \mathbf{F} = &[\xi_1(1,3)\upsilon_{Dr,x} + \xi_2(1,3)\upsilon_{Dr,y}]\left[\phi_{12}, \phi_{22}, 0\right]^{\mathrm{T}} \\ &-[\xi_1(2,3)\upsilon_{Dr,x} + \xi_2(2,3)\upsilon_{Dr,y}]\left[\phi_{11}, \phi_{21}, 0\right]^{\mathrm{T}} \end{aligned} \tag{59}$$

Similarly, when an ellipse rest in two-dimensional uniform velocity gradient stream, the simplified form of formula (55) or (56) is

$$\begin{aligned} \mathbf{F} = &-[m_{12}\upsilon_{Dr,x} + (m_{22} + \bar{m})\upsilon_{Dr,y}]\left[\phi_{12}, \phi_{22}, 0\right]^{\mathrm{T}} \\ &-[(m_{11} + \bar{m})\upsilon_{Dr,x} + m_{12}\upsilon_{Dr,y}]\left[\phi_{11}, \phi_{21}, 0\right]^{\mathrm{T}} \end{aligned} \tag{60}$$

By comparison of the above two formulas, one gets

$$\begin{cases} \xi_1(1,3) = -m_{12}, \quad \xi_2(1,3) = -(m_{22} + \bar{m}) \\ \xi_1(2,3) = m_{11} + \bar{m}, \quad \xi_2(2,3) = m_{12} \end{cases} \tag{61}$$

The analysis above shows that the consistency of Eq. (53) or (54) and Eq. (55) or (56) can be judged by checking the correctness of Eq. (61). We first check the case that the major axis of the ellipse is parallel with Ox. The major axis $a = 1$ m, the minor axis $b = a/\lambda$ where λ is the slenderness ratio and the area of the ellipse is $\bar{m}/\rho = \pi ab$. When the panel number is 640, the panel method shows that $\xi_2(2,3) = \xi_1(1,3) = 0$ and the other numerical result is listed in Table 1.

Comparison with theoretical result shows that the relative error of m_{11}, m_{22} in Table 1 is within 0.04% and indicates the accuracy of the panel method. The theoretical result can be found in Newman (2017) which shows that $m_{11} = \pi\rho b^2, \quad m_{22} = \pi\rho a^2$. The data in Table 1 fulfill Eq. (61) well when the major axis of the ellipse is parallel with Ox and indicates that the formula (53) or (54) is identical with formula (55) or (56).

We now check the case that the major axis is not parallel with the Ox axis. In this case, $\lambda = 4$ and the panel on the ellipse is still 640. The added mass and the generalized added mass under different attack angle α are computed and list in Table 2. The data in Table 2 fulfill Eq. (61) well when the major axis of the ellipse is not parallel with Ox. This again indicates that the formula (53) or (54) is identical with formula (55) or (56).

We now verify formula (53)–(56) with direct numerical simulation result. The direct simulation method of the flow field had been introduced in the previous subsection. To avoid the effect of the boundary and make the uniform velocity gradient field big enough, the length of the two trapezoid bases is doubled. The five points that are adopted to determine the curves are now $(-10, 5), (-5, 4.74), (0, 4.477), (5, 4.25), (10, 4)$. The panel on the ellipse is still 128 but the panel on the trapezoid is now 532. Numerical result shows that $\phi_{11} = -\phi_{22} = 0.0096/\mathrm{s}$,

Table 2
Numerical result of added mass for $\lambda = 4$ ellipse under different attack angle.

$\alpha/°$	0	5	10	15	20	30
$\xi_1(1,3)$/kg	0	−0.2557	−0.5037	−0.7363	−0.9466	−1.2753
$\xi_1(2,3)$/kg	0.9817	1.0041	1.0705	1.1790	1.3263	1.7180
$\xi_2(1,3)$/kg	−3.9269	−3.9046	−3.8381	−3.7297	−3.5824	−3.1906
$\xi_2(2,3)$/kg	0	0.2557	0.5037	0.7363	0.9466	1.2753
m_{11}/kg	0.1963	0.2187	0.2852	0.3936	0.5409	0.9327
m_{12}/kg	0	0.2557	0.5037	0.7363	0.9466	1.2753
m_{22}/kg	3.1416	3.1192	3.0528	2.9443	2.7970	2.4053
$\bar{m}$/kg	0.7854	0.7854	0.7854	0.7854	0.7854	0.7854

Table 3
Hydrodynamic forces for an $a = 1, \lambda = 4$ ellipse.

$\alpha/°$	0	5	10	15	20	30
$F_{x,T}$/N	0.0083	0.0085	0.0090	0.0100	0.0112	0.0145
$F_{y,T}$/N	0	−0.0022	−0.0043	−0.0062	−0.0080	−0.0108
$F_{x,N}$/N	0.0084	0.0086	0.0091	0.0101	0.0113	0.0147
$F_{y,N}$/N	0	−0.0023	−0.0045	−0.0065	−0.0084	−0.0113

$\phi_{12} = \phi_{21} = 0$ and the stream field velocity on the origin is $\mathbf{v}_s(\mathbf{r}_D) = 0.8806\text{m/s}\mathbf{i}$. In the simulation, the center of the ellipse, the origin of the inertial frame and the characteristic point D on the ellipse are all coincident. In this case $\mathbf{v}_{Dr} = -\mathbf{v}_s(\mathbf{r}_D) = -0.8806\,\text{m/s}\mathbf{i}$. According to Eq. (60), the hydrodynamic force acted on the solid is

$$F_{x,T} = -v_{Dr,x}(m_{11} + \bar{m})\phi_{11}, \quad F_{y,T} = -v_{Dr,x}m_{12}\phi_{22} \tag{62}$$

For an ellipse with $a = 1, \lambda = 4$, the exact value of $F_{x,T}, F_{y,T}$ can be determined by substitution of the data in Table 2. When the density $\rho = 1\ \text{kg/m}^2$, the numerical result is listed in the first two lines of Table 3.

Now the ellipse is put into the stream and the disturbed flow field is directly simulated again. After the disturbed flow field is determined, the Bernoulli formula is adopted to determine the pressure distribution on the ellipse and the hydrodynamic force $F_{x,N}, F_{y,N}$ is obtained by integrating the pressure. When the density of the fluid is $\rho = 1\ \text{kg/m}^2$, the numerical result is listed in the last two lines of Table 3. Comparison of the data in Table 3 shows that $F_{x,T} \approx F_{x,N}, F_{y,T} \approx F_{y,N}$. This result shows that the hydrodynamic force formula (53)–(56) is correct when the solid is rest in two-dimensional flow.

3.3. Verification in three dimensional flow

Similarly, we first check the consistency of Eqs. (53)–(56) when the solid is rest. For the case that the major axis is parallel with Ox, the numerical result shows that

$$\begin{cases} \Xi_x = \begin{bmatrix} 0 & 0 & 0 \\ 0 & 0 & \xi_2(1,3) \\ 0 & \xi_3(1,2) & 0 \end{bmatrix} \\ \Xi_y = \begin{bmatrix} 0 & 0 & \xi_1(2,3) \\ 0 & 0 & 0 \\ \xi_3(2,1) & 0 & 0 \end{bmatrix} \\ \Xi_z = \begin{bmatrix} 0 & \xi_1(3,2) & 0 \\ \xi_2(3,1) & 0 & 0 \\ 0 & 0 & 0 \end{bmatrix} \end{cases} \tag{63}$$

for an ellipsoid. The numerical result also verifies the antisymmetric of the matrix $\boldsymbol{\xi}_1, \boldsymbol{\xi}_2, \boldsymbol{\xi}_3$, i.e. $\xi_1(3,2) = -\xi_1(2,3)$, $\xi_2(1,3) = -\xi_2(3,1)$, $\xi_3(2,1) = -\xi_3(1,2)$. The exact value of these non-zero elements is list in Table 4. Substitute the expression of Ξ_x, Ξ_y, Ξ_z, i.e. Eq. (63) into the hydrodynamic force formula (53) or (54), the hydrodynamic force of an ellipsoid resting in uniform velocity gradient three dimensional stream can be rewritten as

$$\mathbf{F} = \begin{bmatrix} \phi_{11}\xi_1(3,2) & \phi_{12}\xi_2(1,3) & \phi_{13}\xi_3(2,1) \\ \phi_{21}\xi_1(3,2) & \phi_{22}\xi_2(1,3) & \phi_{23}\xi_3(2,1) \\ \phi_{31}\xi_1(3,2) & \phi_{32}\xi_2(1,3) & \phi_{33}\xi_3(2,1) \end{bmatrix} \begin{bmatrix} v_{rx} \\ v_{ry} \\ v_{rz} \end{bmatrix} \tag{64}$$

As the major axis of the ellipsoid is parallel with Ox, $m_{12} = m_{13} = m_{23} = 0$ and the hydrodynamic force formula (55) or (56) can be rewritten as

$$\mathbf{F} = \begin{bmatrix} \phi_{11}(m_{11} + \bar{m}) & \phi_{21}(m_{22} + \bar{m}) & \phi_{31}(m_{33} + \bar{m}) \\ \phi_{12}(m_{11} + \bar{m}) & \phi_{22}(m_{22} + \bar{m}) & \phi_{32}(m_{33} + \bar{m}) \\ \phi_{13}(m_{11} + \bar{m}) & \phi_{23}(m_{22} + \bar{m}) & \phi_{33}(m_{33} + \bar{m}) \end{bmatrix} \begin{bmatrix} v_{br,x} \\ v_{br,y} \\ v_{br,z} \end{bmatrix} \tag{65}$$

Comparison of the two equations above shows that

$$\xi_1(3,2) = -(m_{11} + \bar{m}), \quad \xi_2(1,3) = -(m_{22} + \bar{m}), \quad \xi_3(2,1) = -(m_{33} + \bar{m}) \tag{66}$$

The analysis above shows that the consistency of Eq. (53) or (54) and Eq. (55) or (56) can be judged by checking the correctness of Eq. (65). Similarly, we first check the case that the major axis of the ellipsoid is parallel with Ox. The minor axis $b = 1$ m, the major axis $a = b\lambda$ where λ is the slenderness ratio and the volume of the ellipsoid is $\bar{m}/\rho = 4\pi ab^2/3$. As $m_{22} = m_{33}$ for an axisymmetric ellipsoid and numerical result shows that $\xi_3(2,1) = \xi_2(1,3)$, we need only to check the correctness of the first two identities in Eq. (66). When $\rho = 1\ \text{kg/m}^3$ and the panel number is 900, the numerical result of $\bar{m}$ and the added mass is listed in Table 5. To check the correctness of Eq. (66), two relative error $RE_1 = [\frac{\bar{m}+m_{11}}{-\xi_1(3,2)} - 1] \times 100$ and $RE_2 = [\frac{\bar{m}+m_{22}}{-\xi_2(1,3)} - 1] \times 100$ is calculated and also list in Table 5. It can be seen from Table 5 that both RE_1 and RE_2 are small. Consequently, Eq. (66) is verified and the identity between Eq. (53) or (54) and Eq. (55) or (56) can be asserted when the solid is rest.

Now we verify the correctness of the hydrodynamic force formulas (53)–(54) with direct simulation results. The computation of the three-dimensional panel method is much more complex than that of the two-dimensional flow. Thus, the panel number should be reduced to save computation time. According to the study in two-dimensional flow simulation, the outer trapezoid boundary had costed most panels. Consequently, the Newman hypothesis (4) is adopted so that the panel is distributed on the ellipsoid only to compute $\mathbf{v}$. The parameter of $\mathbf{v}_s$ in Eq. (1) are $\mathbf{r}_R = [0,0,0]^{\mathrm{T}}, \mathbf{v}_s(\mathbf{r}_R) = [0,0,0]^{\mathrm{T}}$. The translating velocity $\mathbf{v}_{Dr}$ and the velocity gradient are

$$v_{Dr} = \begin{bmatrix} v_{Dr,x} \\ v_{Dr,y} \\ 0 \end{bmatrix}, \quad \boldsymbol{\Phi} = \begin{bmatrix} \phi_{11} & \phi_{12} & 0 \\ \phi_{12} & -\phi_{11}/2 & 0 \\ 0 & 0 & -\phi_{11}/2 \end{bmatrix} \tag{67}$$

Table 4
Numerical result of added mass for an ellipsoid.

λ	1.5	2	2.5	3	4	5
$\xi_1(2,3)$	8.0929	10.0113	11.9568	13.9224	17.8962	21.9093
$\xi_2(3,1)$	10.1580	14.2422	18.4167	22.6377	31.1395	39.6659
$\xi_3(1,2)$	10.0658	14.1159	18.2543	22.4368	30.8557	39.2922

Table 5
Numerical result of $\bar{m}$ and added mass for ellipsoids.

λ	1.5	2	2.5	3	4	5
m_{11}	1.8755	1.7215	1.5945	1.4875	1.3170	1.1846
m_{22}	3.8902	5.8835	7.9660	10.0939	14.4061	18.7401
$\xi_1(3,2)$	−8.0929	−10.0113	−11.9568	−13.9224	−17.8962	−21.9093
$\xi_2(1,3)$	−10.0658	−14.1159	−18.2543	−22.4368	−30.8557	−39.2922
$\bar{m}$	6.2832	8.3776	10.4720	12.5664	16.7552	20.9440
RE_1	0.8131	0.8770	0.9175	0.9445	0.9834	1.0009
RE_2	1.0690	1.0286	1.0063	0.9961	0.9904	0.9974

Table 6
Hydrodynamic forces for an $\lambda = 4$ ellipsoid.

$v_{Dr,y}$/m/s	0	0.1	0.2	0.3	0.4	0.5
$F_{x,T}$/N	0.1812	0.2435	0.3059	0.3682	0.4305	0.4928
$F_{y,T}$/N	0.3624	0.3469	0.3313	0.3157	0.3001	0.2845
$F_{x,N}$/N	0.1792	0.2414	0.3037	0.3659	0.4281	0.4904
$F_{y,N}$/N	0.3584	0.3427	0.32 705	0.3113	0.2956	0.2799

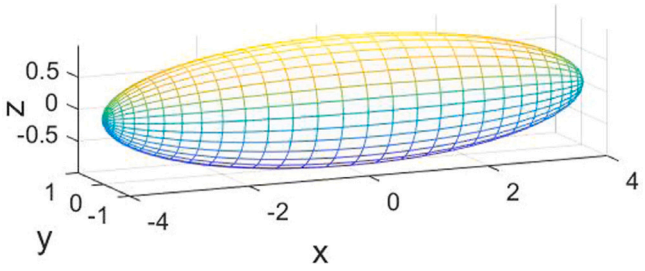

Fig. 3. The grid distribution on the ellipsoid.

where $v_{Dr,x} = 1\text{m/s}, \phi_{11} = \phi_{12}/2 = 0.01/\text{s}$. Though the major axis is parallel with Ox, the direction of $\mathbf{v}_{Dr}$ changes with the variation of $v_{Dr,y}$ and the attack angle of the ellipsoid is not necessarily zero. According to the description of these parameters, Eq. (65) can be simplified as

$$\begin{cases} F_{x,T} = \phi_{11}(m_{11} + \bar{m})v_{br,x} + \phi_{21}(m_{22} + \bar{m})v_{br,y} \\ F_{y,T} = \phi_{12}(m_{11} + \bar{m})v_{br,x} + \phi_{22}(m_{22} + \bar{m})v_{br,y} \end{cases} \tag{68}$$

The exact value of $F_{x,T}, F_{y,T}$ can be determined by substituting the data in Table 5. For a $a = 4$ m, $b = 1$ m ellipsoid, when the density of the fluid is $\rho = 1$ kg/m^3, the numerical result is listed in the first two lines in Table 6 Then, the direct simulation method is adopted to compute the two components $F_{x,N}$ and $F_{y,N}$ of the hydrodynamic force. The $\mathbf{v}_s$ in Eq. (4) is determined now. The $\mathbf{v}$ in Eq. (4) is the induced flow field by the same ellipsoid translating with velocity $[v_{Dr,x}, v_{Dr,y}, 0]^{\mathrm{T}}$ in non-stream field and can be determined by panel method. When the disturbed flow field $\mathbf{v}_w$ is determined according to Eq. (4), the hydrodynamic force cannot be determined by applying Bernoulli's formula and integrating the pressure. In the direct numerical study in two-dimensional flow, the velocity in the far-field is uniform and the Bernoulli's formula is applicable. In the study of three-dimensional flow introduced just now, the velocity in the far-field is not uniform and Eq. (7) should be adopted to evaluate the hydrodynamic force. In fact, it can be seen from Eq. (7) that Bernoulli's formula accounts only for the last term. The first term of Eq. (7) accounts for the unsteady effect of the flow field. The second term of Eq. (7) accounts for the non-uniform effect of the far flow field. For a $a = 4$ m, $b = 1$ m ellipsoid, the panel is illustrated in Fig. 3 when the total number is 900. The numerical result $F_{x,N}, F_{y,N}$ is list in the last two lines of Table 6 when the fluid density $\rho = 1$ kg/m^3. It can be seen from Table 6 that the numerical result $F_{x,N}, F_{y,N}$ is quite close to the theoretical result $F_{x,T}, F_{y,T}$. This result verifies the correctness of Eqs. (53)–(54) when the ellipsoid is rest.

3.4. Verification in the solid translating circumstance

As Eqs. (53)–(56) are identical when the solid is resting, we are going to verify the correctness of Eq. (56) only when the solid is translating. For simplicity, the solid is an axisymmetric ellipsoid with $a = 4$ m, $b = 1$ m and the major axis parallel with Ox. At the $t = 0$ moment, the center of the ellipsoid is coincident with the origin of the inertial frame and the translating velocity is zero. Then, the ellipsoid starts to translate in Ox direction with uniform acceleration $a = 1$ m/s^2. The velocity varies with time by $v_{D,x} = at$ and the position on Ox coordinate varies with time by $x_D = 0.5at^2$. The velocity gradient of the stream $\boldsymbol{\Phi}$ still have the form of Eq. (67) and $\phi_{11} = 0.01/\text{s}, \phi_{12} = 0/\text{s}$, The parameters in Eq. (1) is $\mathbf{r}_R = 0$, $\mathbf{v}_s(\mathbf{r}_R) = 0$ and

$$v_{Dr,x} = v_{D,x} - v_{s,x}(\mathbf{r}_D) = v_{D,x} - x_D\phi_{11} = at - 0.5at^2\phi_{11} \tag{69}$$

Substitute the above parameters in Eq. (56), the resultant hydrodynamic force has only Ox component with

$$\begin{aligned} F_x &= \phi_{11}(\bar{m} + m_{11})at - m_{11}a - \phi_{11}(\bar{m} + m_{11})(at - 0.5at^2\phi_{11}) \\ &= -m_{11}a + \phi_{11}(\bar{m} + m_{11})at^2/2 \end{aligned} \tag{70}$$

The variation of F_x with time t is illustrated in Fig. 4 with blue dots.

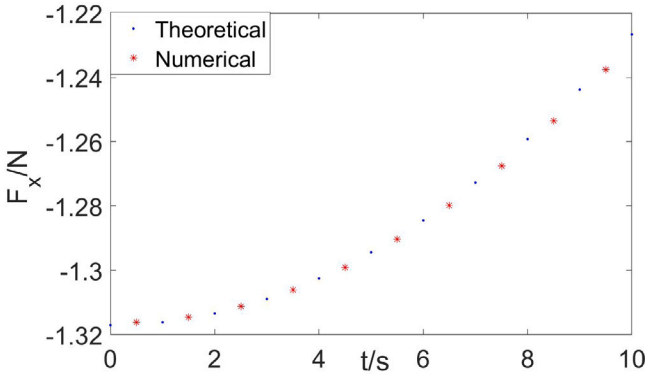

Fig. 4. Comparison of the hydrodynamic force between theoretical and numerical result when the ellipsoid is translating.

Then the hydrodynamic force is computed directly. The uniform gradient stream $\mathbf{v}_s$ had been described in the previous paragraph. The disturbed flow field $\mathbf{v}$ induced by the ellipsoid translating with velocity $\mathbf{v}_{D,r} = (at - 0.5at^2\phi_{11})\mathbf{i}$ in non-stream field is computed by panel method. The disturbed flow field $\mathbf{v}_w$ by the ellipsoid translating in the uniform gradient stream is acquired by summing up $\mathbf{v}_s$ and $\mathbf{v}$ according to the Newman hypothesis (4). As the panel method can only compute the $\mathbf{v}$ on the specified moment, the determination of $\mathbf{v}_w(t)$ requires repeatedly applying the panel method on different moments. At last, the hydrodynamic force is evaluated according to formula (7) and the numerical result is plotted in Fig. 4 with red stars. Fig. 4 clearly shows that the numerical result is coincident with the theoretical prediction and verifies the correctness of Eq. (56) when the solid is translating.

4. Observation

This section discusses the compatibility of the newly acquired hydrodynamic force formula with the previous study, including the hydrodynamic force formula provided by Taylor, Newman, and Thomasson.

4.1. Comparison with the study of Taylor

When the solid is resting in the uniform gradient stream, the study by Taylor (1928)(equ(6)) shew that the hydrodynamic force acted on it is

$$\begin{cases} F_x = \frac{1}{2}\rho V_b \frac{\partial}{\partial x}(u^2 + v^2 + w^2) + \frac{\partial T}{\partial u}\frac{\partial u}{\partial x} + \frac{\partial T}{\partial v}\frac{\partial v}{\partial x} + \frac{\partial T}{\partial w}\frac{\partial w}{\partial x} \\ F_y = \frac{1}{2}\rho V_b \frac{\partial}{\partial y}(u^2 + v^2 + w^2) + \frac{\partial T}{\partial u}\frac{\partial u}{\partial y} + \frac{\partial T}{\partial v}\frac{\partial v}{\partial y} + \frac{\partial T}{\partial w}\frac{\partial w}{\partial y} \\ F_z = \frac{1}{2}\rho V_b \frac{\partial}{\partial z}(u^2 + v^2 + w^2) + \frac{\partial T}{\partial u}\frac{\partial u}{\partial z} + \frac{\partial T}{\partial v}\frac{\partial v}{\partial z} + \frac{\partial T}{\partial w}\frac{\partial w}{\partial z} \end{cases} \tag{71}$$

with

$$2T/\rho = m_{11}u^2 + m_{22}v^2 + m_{33}w^2 + 2m_{23}vw + 2m_{13}wu + 2m_{12}uv \tag{72}$$

where $u = v_{s,x}(\mathbf{r}_D), v = v_{s,y}(\mathbf{r}_D), w = v_{s,z}(\mathbf{r}_D)$ is the three velocity components of the stream at the center of the solid respectively. Let

$\mathbf{v}_D = 0$ in Eq. (56), it can be easily found that its scaler form is the same as Eq. (71). This in some sense verify the correctness of Eqs. (53)–(56). However, the formula provided by Taylor is only applicable in the case that the solid is resting while the hydrodynamic force formulas (53)–(56) proposed in this study are applicable in both solid resting and translating circumstances.

Though Taylor claimed to had acquired equation (71) by two methods, only one method is illustrated. This illustrated method is only a direct generalization of the hydrodynamic force acting on a sphere and is not rigidly proved for arbitrary formed solid. What is more, The following energy formula claimed to have been proposed by Lord Kelvin is adopted in the proof of the hydrodynamic force acting on the sphere.

$$T = K + \frac{1}{2}(M + m_{11})(v_{D,x}^2 + v_{D,y}^2 + v_{D,z}^2) \tag{73}$$

However, Taylor did not clarify the quoting reference of Lord Kelvin's study. Comparatively, the proof provided in this study is rigid and detailed.

Taylor's study is base on the complex Lagrangian mechanics and the hydrodynamic force is determined by the relationship that the work acted on the fluid by the solid equals to the variation of the fluid kinetic energy. Comparatively, the Newtonian mechanics is easier to understand. To study the hydrodynamic force basing on the momentum conservation based Newtonian mechanics, a control volume should be drawn in the flow field first. Then the total momentum in the control volume and the total pressure on the control volume boundary should be evaluated. However, the analytical evaluation of these two variables is not easy even when the radius of the control volume is extended to infinity. It had long been realized by the hydrodynamics pioneers and is also confirmed by modern scholars that the total momentum in an infinitely large control volume is indeterminate (Lamb, 1945; Batchelor, 1967; Wu et al., 2015). The total pressure on the control volume boundary was supposed to be zero by the hydrodynamics pioneers (Lamb, 1945; Calero, 2018) but is found to be incorrect by modern scholars (Wu, 2014:). The complexity of the control volume momentum and the total boundary pressure prevents the earlier scholars to adopt the simpler Newtonian mechanics. In the 1990s, the pressure elimination method was rediscovered by Noca et al. (1997, 1999) and make the study on hydrodynamic force basing on Newtonian mechanics possible. In fact, this technology had been found by the previous scholars and had been adopted by Newman in inviscid flow in 1970s to study the hydrodynamic force. This study will be analyzed in the next subsection.

4.2. Comparison with Newman's result

Newman used the Euler equation to eliminate the pressure on the control volume's outer boundary and the following hydrodynamic force formula was proposed

$$\mathbf{F}_w = -\rho\frac{\mathrm{d}}{\mathrm{d}t}\int_{S_i}\phi_w \mathrm{d}S - \rho\int_{S_e}\left(\frac{\partial\phi}{\partial n}\nabla\phi_w - \frac{\mathbf{n}}{2}\nabla\phi_w\cdot\nabla\phi_w\right)\mathrm{d}S \tag{74}$$

where ϕ_w is the potential of $\mathbf{v}_w$. Basing on this formula and his hypothesis (4), the following hydrodynamic force formula is acquired

$$\begin{aligned} F_x &= -m_{11}\frac{\mathrm{d}U_1}{\mathrm{d}t} - (m_{11}+\bar{m})\frac{\partial p_s}{\partial x} \\ &= -m_{11}\frac{\mathrm{d}v_{D,x}}{\mathrm{d}t} + (\bar{m}+m_{11})v_{s,x}(\mathbf{r}_D)\frac{\partial v_{s,x}(\mathbf{r}_D)}{\partial x} \end{aligned} \tag{75}$$

where p_s is the distribution of the pressure in the undisturbed stream. The first term represents the hydrodynamic force due to the acceleration of the solid. The second term represents the hydrodynamic force of the solid resting in the stream. The comparison shows that the equation above is compatible with Eqs. (53)–(56) but is only applicable when the solid is axisymmetric and its axis is parallel with the local stream.

Though Newman's formula (75) is correct, some flaws exist in its derivation process. The main skill in Newman's derivation is to construct a complex vector

$$\begin{aligned} \mathbf{A} = &-\frac{\partial\Psi_s}{\partial z}\frac{\partial}{\partial x}\left(\frac{1}{r}\right) + \frac{1}{r}\frac{\partial^2\Psi_s}{\partial x\partial z} - \frac{\partial\Psi_s}{\partial x}\frac{\partial}{\partial z}\left(\frac{1}{r}\right)\mathbf{j} \\ &+\frac{\partial\Psi_s}{\partial y}\frac{\partial}{\partial x}\left(\frac{1}{r}\right) - \frac{1}{r}\frac{\partial^2\Psi_s}{\partial x\partial y} + \frac{\partial\Psi_s}{\partial x}\frac{\partial}{\partial y}\left(\frac{1}{r}\right)\mathbf{k} \end{aligned} \tag{76}$$

and found the following identity

$$\begin{aligned} &(\nabla\times\mathbf{A})\cdot\mathbf{n} + \frac{\partial^2\Psi_s}{\partial x^2}\frac{\partial}{\partial n}\left(\frac{1}{r}\right) - \frac{1}{r}\frac{\partial}{\partial n}\frac{\partial^2\Psi_s}{\partial x^2} \\ &= n_x\nabla\Psi_s\cdot\nabla\left[\frac{\partial}{\partial x}\left(\frac{1}{r}\right)\right] - \frac{\partial^2}{\partial x^2}\left(\frac{1}{r}\right)\frac{\partial\Psi_s}{\partial n} - \frac{\partial\Psi_s}{\partial x}\frac{\partial^2}{\partial n\partial x}\left(\frac{1}{r}\right) \end{aligned} \tag{77}$$

The Ψ_s in the two equations above is the potential of the stream velocity $\mathbf{v}_s$. $\mathbf{A}$ is so complex that it is difficult to be extended to the cases that the solid is not axisymmetric. This may be the reason why the more general hydrodynamic force formula is not proposed by Newman.

In Newman's study (Newman, 2017), the right side of Eq. (77) is reversed. Ignoring this typo, the following hydrodynamic force formula can be acquired by Newman's method

$$F_x = (\bar{m}+m_{11})\left\{\frac{\mathrm{d}v_{s,x}(\mathbf{r}_D)}{\mathrm{d}t} + [v_{s,x}(\mathbf{r}_D) - v_{D,x}]\frac{\partial v_{s,x}(\mathbf{r}_D)}{\partial x}\right\} - m_{11}\frac{\mathrm{d}v_{D,x}}{\mathrm{d}t} \tag{78}$$

As $\mathrm{d}v_{s,x}(\mathbf{r}_D)/\mathrm{d}t = v_{D,x}\partial v_{s,x}/\partial x$ according to Eq. (34), the terms in the brace can be simplified as $v_{s,x}(\mathbf{r}_D)\partial v_{s,x}(\mathbf{r}_D)/\partial x$. As the stream is steady, this term is exactly $-\partial p_s/\partial x$ according to the Euler equation. Finally one gets

$$F_x = -(\bar{m}+m_{11})\frac{\partial p_s}{\partial x} - m_{11}\frac{\mathrm{d}v_{D,x}}{\mathrm{d}t} \tag{79}$$

This hydrodynamic force formula is identical to that acquired by Newman, however, the derivation process is different.

In Newman's study, the terms in the brace of Eq. (78) is

$$B = \frac{\partial v_{s,x}(\mathbf{r}_D)}{\partial t} + [v_{s,x}(\mathbf{r}_D) - v_{D,x}]\frac{\partial v_{s,x}(\mathbf{r}_D)}{\partial x} \tag{80}$$

Then Newman claimed that $B = -\partial p_s/\partial x$ if the Euler equation is rewritten in a coordinate system translating with the body velocity $v_{D,x}$. There are two errors in this process. Firstly, the first term of B is $\mathrm{d}v_{s,x}(\mathbf{r}_D)/\mathrm{d}t$ but not $\partial v_{s,x}(\mathbf{r}_D)/\partial t$. Secondly, $B = -v_{D,x}\partial v_{s,x}(\mathbf{r}_D)/\partial x - \partial p_s/\partial x$ by applying the Euler equation and noticing that $\partial v_{s,x}(\mathbf{r}_D)/\partial t = 0$. As $v_{D,x}\partial v_{s,x}(\mathbf{r}_D)/\partial x \neq 0$, Newman's hydrodynamic force formula (79) cannot be acquired according to Newman's derivation process.

4.3. Comparison with the study of Thomasson

In 2013, the dynamical equation for a solid moving in the unsteady and non-uniform stream had been proposed by Thomasson and Woolsey (2013). The hydrodynamic force $\mathbf{F}_A$ and moment $\mathbf{M}_A$ acted on the solid can be clarified by moving the terms that are proportional to the fluid density to the right side of the equation. The result shows that

$$\begin{aligned} &\begin{bmatrix}\mathbf{F}_A\\ \mathbf{M}_A\end{bmatrix} = -\mathcal{M}_f\begin{bmatrix}\dot{\mathbf{v}}_D - \dot{\mathbf{v}}_u - \dot{\mathbf{v}}_s\\ \dot{\boldsymbol{\omega}}_b\end{bmatrix} - \begin{bmatrix}\hat{\boldsymbol{\omega}}_b & \mathbf{0}\\ \hat{\mathbf{v}}_r & \hat{\boldsymbol{\omega}}_b\end{bmatrix}(\mathcal{M}_f + \bar{\mathcal{M}})\begin{bmatrix}\mathbf{v}_{Dr}\\ \boldsymbol{\omega}_b\end{bmatrix} \\ &+\begin{bmatrix}\hat{\boldsymbol{\omega}}_b & \mathbf{0}\\ \hat{\mathbf{v}}_r + \hat{\mathbf{v}}_u + \hat{\mathbf{v}}_s & \hat{\boldsymbol{\omega}}_b\end{bmatrix}\bar{\mathcal{M}}\begin{bmatrix}\mathbf{v}_u + \mathbf{v}_s\\ \mathbf{0}\end{bmatrix} + \begin{bmatrix}\mathbf{0} & \mathbf{0}\\ \hat{\mathbf{v}}_u + \hat{\mathbf{v}}_s & \mathbf{0}\end{bmatrix}\bar{\mathcal{M}}\begin{bmatrix}\mathbf{v}_{Dr}\\ \boldsymbol{\omega}_b\end{bmatrix} \\ &+\bar{\mathcal{M}}\begin{bmatrix}(\hat{\mathbf{v}}_u + \hat{\mathbf{v}}_s)\boldsymbol{\omega}_b + \frac{\partial\mathbf{v}_u}{\partial t} + \boldsymbol{\Phi}^{\mathrm{T}}(\mathbf{v}_{Dr} + \mathbf{v}_u + \mathbf{v}_s)\\ \mathbf{0}\end{bmatrix} \\ &-\begin{bmatrix}\boldsymbol{\Phi} & \mathbf{0}\\ \mathbf{0} & \mathbf{0}\end{bmatrix}(\mathcal{M}_f + \bar{\mathcal{M}})\begin{bmatrix}\mathbf{v}_{Dr}\\ \boldsymbol{\omega}_b\end{bmatrix} \end{aligned} \tag{81}$$

where

$$\mathcal{M}_f = \begin{bmatrix} \mathbf{M}_{FV} & \mathbf{M}_{F\omega} \\ \mathbf{M}_{MV} & \mathbf{M}_{M\omega} \end{bmatrix}, \quad \bar{\mathcal{M}} = \begin{bmatrix} \bar{m}\mathbf{I} & \mathbf{0} \\ \mathbf{0} & \mathbf{0} \end{bmatrix} \tag{82}$$

and $\mathbf{M}_{FV}, \mathbf{M}_{F\omega}, \mathbf{M}_{MV}, \mathbf{M}_{M\omega}$ is the four block matrix of the added mass. Under the hypothesis of this study, $\mathbf{v}_u = 0, \dot{\mathbf{v}}_s = 0, \boldsymbol{\omega}_b = 0$. In this case the hydrodynamic force can be simplified as

$$\begin{aligned} \mathbf{F}_A &= -\mathbf{M}_{FV}\dot{\mathbf{v}}_D + \bar{m}\boldsymbol{\Phi}^{\mathrm{T}}(\mathbf{v}_{Dr} + \mathbf{v}_s) - \boldsymbol{\Phi}(\mathbf{M}_{FV} + \bar{m}\mathbf{I})\mathbf{v}_{Dr} \\ &= -\mathbf{M}_{FV}\dot{\mathbf{v}}_D + \bar{m}\boldsymbol{\Phi}^{\mathrm{T}}\mathbf{v}_s - \boldsymbol{\Phi}\mathbf{M}_{FV}\mathbf{v}_{Dr} = -\mathbf{M}_{FV}\dot{\mathbf{v}}_D - \boldsymbol{\Phi}(\mathbf{M}_{FV} + \bar{m}\mathbf{I})\mathbf{v}_{Dr} \end{aligned} \tag{83}$$

It is not supposed that $\boldsymbol{\Phi}^{\mathrm{T}} = \boldsymbol{\Phi}$ in Thomasson and Woolsey (2013). However, its final result should also be applicable in the case that $\boldsymbol{\Phi}^{\mathrm{T}} = \boldsymbol{\Phi}$. Consequently, this identity had been applied on the final equal of the equation above. Transform our hydrodynamic force formula (56) into matrix form, one gets

$$\mathbf{F} = (\bar{m}\mathbf{I} + \mathbf{M}_{FV})\boldsymbol{\Phi}\mathbf{v}_D - \mathbf{M}_{FV}\dot{\mathbf{v}}_D - \boldsymbol{\Phi}(\bar{m}\mathbf{I} + \mathbf{M}_{FV})\mathbf{v}_{Dr} \tag{84}$$

By comparison of the two equations above, one can see that Thomasson's result is diffident from our result.

It is difficult to figure out the error in the study of Thomasson and Woolsey (2013) exactly as the process is so complex. However, we can compare the kinetic energy expression proposed there with that of Taylor (1928). In the special case that the stream is steady, the kinetic energy of a sphere moving in the stream according to Thomasson's study should be

$$\begin{aligned} T = K + \frac{1}{2}(\bar{m} + m_{11})[(v_{D,x} - v_{s,x})^2 + (v_{D,y} - v_{s,y})^2 \\ +(v_{D,z} - v_{s,z})^2] + \frac{1}{2}(M - \bar{m})(v_{D,x}^2 + v_{D,x}^2 + v_{D,x}^2) \end{aligned} \tag{85}$$

where M is the mass of the sphere. Comparison with Eq. (73) shows that the kinetic energy expression above is not consistent with those adopted by Taylor. This fact not only points out one of the possible reason why Thomasson's result is not consistent with the present study, but also indicates the complex of the Lagrangian mechanics and the necessity of Newtonian mechanics adopted in this study.

5. Conclusions

The hydrodynamic force formulas for a solid translating in a uniform gradient stream is derived based on Newtonian Mechanics. The main conclusions of this study are

(a) The hydrodynamic force can be predicted according to Eqs. (53)–(56) as long as the translating velocity of the solid, the relative velocity of the solid, the gradient of the stream, and the added mass are given.

(b) The derivation of the hydrodynamic force formula can be simplified if the concept of the generalized added mass (12) is adopted. The matrix of the generalized tensors are all antisymmetric matrixes.

(c) The added mass can be computed based on the new proposed velocity-vector based formula (11) or (16) and (17) and the classical Hess & Smith panel method.

(d) These new formulas are compatible with both the classical Taylor formula which is valid for the resting solid and the Newman formula which is valid for axisymmetric and zero attack angle translating solid.

(e) Comparing with the kinetic energy conservation theorem based classical Lagrangian Mechanics proof, this momentum conservation theorem based Newtonian Mechanics proof is not only rigid but also extendable for viscous flow.

CRediT authorship contribution statement

Xianwu Lin: Conceptualization, Methodology, Software, Validation, Formal analysis, Investigation, Data curation, Writing – original draft, Writing – review & editing, Visualization, Funding acquisition. **Lixun Xiong:** Software, Data curation, Visualization, Writing – review & editing.

Declaration of competing interest

The authors declare that they have no known competing financial interests or personal relationships that could have appeared to influence the work reported in this paper.

Appendix

A.1. DMT formula and vector identities

The following Derivative Moment Transformation (DMT) formula had been quoted in the paper. The detailed proof of these formulas can be found in Ref. Wu et al. (2015). For a closed surface S, let $\mathbf{n}$ be its outwards normal, N be the dimension of the flow field, ϕ is a continuous scalar field, $\mathbf{r}$ is the position vector of the flow field referencing to an arbitrary point, then

$$-\int_S \phi\mathbf{n}\mathrm{d}S = \frac{1}{N-1}\int_S \mathbf{r}\times(\mathbf{n}\times\nabla\phi)\mathrm{d}S, \ N = 2,3 \tag{86}$$

Let R be a region of the flow field enclosed by S and $\mathbf{F}$ be a continuous vector field, then

$$\int_R \mathbf{F}\mathrm{d}R = \frac{1}{N-1}\int_R \mathbf{r}\times(\nabla\times\mathbf{F})\mathrm{d}R + \frac{1}{N-1}\int_S \mathbf{r}\times(\mathbf{F}\times\mathbf{n})\mathrm{d}S, \ N = 2,3 \tag{87}$$

$$\int_S \mathbf{r}\times\mathbf{n}\phi\mathrm{d}S = \frac{1}{2}\int_S x^2\mathbf{n}\times(\nabla\phi)\mathrm{d}S, \ N = 2,3 \tag{88}$$

$$2\int_R \mathbf{r}\times\mathbf{F}\mathrm{d}R = -\int_R r^2\nabla\times\mathbf{F}\mathrm{d}R + \int_S r^2\mathbf{n}\times\mathbf{F}\mathrm{d}S, \ N = 2,3 \tag{89}$$

The following algebraic identity is also used in the paper (Wu, 2014:)

$$\nabla(\mathbf{F}\cdot\mathbf{G}) = (\mathbf{F}\cdot\nabla)\mathbf{G} + (\mathbf{G}\cdot\nabla)\mathbf{F} + \mathbf{G}\times(\nabla\times\mathbf{F}) + \mathbf{F}\times(\nabla\times\mathbf{G}) \tag{90}$$

$$\nabla\times(\phi\mathbf{F}) = \nabla\phi\times\mathbf{F} + \phi\nabla\times\mathbf{F} \tag{91}$$

as well as the formula for evaluating the divergency of dyad

$$\nabla\cdot(\mathbf{F}\mathbf{G}) = (\mathbf{F}\cdot\nabla)\mathbf{G} + (\nabla\cdot\mathbf{F})\mathbf{G} \tag{92}$$

A.2. Proof of Eq. (46)

A.2.1. Proof in two dimensional flow

For two dimensional flow, Eq. (46) can be rewritten as

$$\int_{R_b'-R_b} \mathbf{r}\cdot\boldsymbol{\Phi}\times\boldsymbol{\omega}_1\mathrm{d}V = -\int_{R_b'-R_b} \boldsymbol{\Phi}\cdot(\mathbf{r}\times\boldsymbol{\omega}_1)\mathrm{d}V \tag{93}$$

The equation above can be proved by verifying $\mathbf{r}\cdot\boldsymbol{\Phi}\times\boldsymbol{\omega}_1 = -\boldsymbol{\Phi}\cdot(\mathbf{r}\times\boldsymbol{\omega}_1)$. The matrix form of $\mathbf{r}\cdot\boldsymbol{\Phi}\times\boldsymbol{\omega}_1$ is $-\tilde{\boldsymbol{\omega}}\boldsymbol{\Phi}^T\mathbf{r}$, the matrix form of $-\boldsymbol{\Phi}\cdot(\mathbf{r}\times\boldsymbol{\omega}_1)$ is $\boldsymbol{\Phi}^T\tilde{\boldsymbol{\omega}}\mathbf{r}$. Further noticing that $\boldsymbol{\Phi}^T = \boldsymbol{\Phi}$, one finds that the vector identity $\mathbf{r}\cdot\boldsymbol{\Phi}\times\boldsymbol{\omega}_1 = -\boldsymbol{\Phi}\cdot(\mathbf{r}\times\boldsymbol{\omega}_1)$ is equivalent to the matrix identity $\boldsymbol{\Phi}\tilde{\boldsymbol{\omega}} = -\tilde{\boldsymbol{\omega}}\boldsymbol{\Phi}$. This matrix identity further result in $(\boldsymbol{\Phi}\tilde{\boldsymbol{\omega}})^{\mathrm{T}} = \tilde{\boldsymbol{\omega}}^{\mathrm{T}}\boldsymbol{\Phi}^{\mathrm{T}} = -\tilde{\boldsymbol{\omega}}\boldsymbol{\Phi} = \boldsymbol{\Phi}\tilde{\boldsymbol{\omega}}$. The discussion above shows that, Eq. (93) can be proved by showing that $\boldsymbol{\Phi}\tilde{\boldsymbol{\omega}}$ is a symmetric matrix.

Noticing the symmetric of matrix $\boldsymbol{\Phi}$ as shown in the discussion followed Eq. (2) and the anti-symmetry of matrix $\tilde{\boldsymbol{\omega}}$ as shown in Eq. (20), the components of $\boldsymbol{\Phi}\tilde{\boldsymbol{\omega}}$ can be clarified as

$$\boldsymbol{\Phi}\tilde{\boldsymbol{\omega}} = \begin{bmatrix} \phi_{12}\omega_3 - \phi_{13}\omega_2 & \phi_{13}\omega_1 - \phi_{11}\omega_3 & \phi_{11}\omega_2 - \phi_{12}\omega_1 \\ \phi_{22}\omega_3 - \phi_{23}\omega_2 & \phi_{23}\omega_1 - \phi_{12}\omega_3 & \phi_{12}\omega_2 - \phi_{22}\omega_1 \\ \phi_{23}\omega_3 - \phi_{33}\omega_2 & \phi_{33}\omega_1 - \phi_{13}\omega_3 & \phi_{13}\omega_2 - \phi_{23}\omega_1 \end{bmatrix} \tag{94}$$

To ensure that $\boldsymbol{\Phi}\tilde{\boldsymbol{\omega}}$ is symmetric, it required that

$$\begin{cases} \phi_{22}\omega_3 - \phi_{23}\omega_2 = \phi_{13}\omega_1 - \phi_{11}\omega_3 \\ \phi_{12}\omega_2 - \phi_{22}\omega_1 = \phi_{33}\omega_1 - \phi_{13}\omega_3 \\ \phi_{23}\omega_3 - \phi_{33}\omega_2 = \phi_{11}\omega_2 - \phi_{12}\omega_1 \end{cases} \tag{95}$$

For two dimensional flow $\omega_1 = \omega_2 = 0, \phi_{13} = \phi_{23} = 0$. In this case, Eq. (95) can be simplified as $\phi_{22}\omega_3 = -\phi_{11}\omega_3$ and is obviously true for incompressible two dimensional flow. The discussion above shows that $\boldsymbol{\Phi}\tilde{\boldsymbol{\omega}}$ is indeed a symmetric matrix in two dimensional flow. Consequently, $\mathbf{r}\cdot\boldsymbol{\Phi}\times\boldsymbol{\omega}_1 = -\boldsymbol{\Phi}\cdot(\mathbf{r}\times\boldsymbol{\omega}_1)$ and Eq. (93) is proved.

A.2.2. Proof in three dimensional flow

For three dimensional flow, Eq. (46) become

$$\int_{R_b'-R_b} \mathbf{r}\cdot\boldsymbol{\Phi}\times\boldsymbol{\omega}_1 \mathrm{d}V = -\frac{1}{2}\int_{R_b'-R_b} \boldsymbol{\Phi}\cdot(\mathbf{r}\times\boldsymbol{\omega}_1)\mathrm{d}V \tag{96}$$

Let $\boldsymbol{\Delta}_1 = \mathbf{r}\cdot\boldsymbol{\Phi}\times\boldsymbol{\omega}_1 + \boldsymbol{\Phi}\cdot(\mathbf{r}\times\boldsymbol{\omega}_1)/2$ and transform $\boldsymbol{\Delta}_1$ into scaler form, one gets

$$\begin{aligned} \Delta_{1,x} &= \phi_{22}(\omega_{1,z}y + \omega_{1,y}z)/2 - \phi_{33}(\omega_{1,y}z + \omega_{1,z}y)/2 \\ &+\phi_{12}(\omega_{1,z}x + \omega_{1,x}z)/2 - \phi_{13}(\omega_{1,y}x + \omega_{1,x}y)/2 + \phi_{23}(\omega_{1,z}z - \omega_{1,y}y) \end{aligned} \tag{97}$$

$$\begin{aligned} \Delta_{1,y} &= \phi_{22}(\omega_{1,z}x + \omega_{1,x}z)/2 + \phi_{33}(\omega_{1,x}z + \omega_{1,z}x) \\ &-\phi_{12}(\omega_{1,z}y + \omega_{1,y}z)/2 + \phi_{13}(\omega_{1,x}x - \omega_{1,z}z) + \phi_{23}(\omega_{1,y}x + \omega_{1,x}y) \end{aligned} \tag{98}$$

$$\begin{aligned} \Delta_{1,z} &= -\phi_{22}(\omega_{1,y}x + \omega_{1,x}y)/2 - \phi_{33}(\omega_{1,y}x + \omega_{1,x}y) \\ &+\phi_{12}(\omega_{1,y}y - \omega_{1,x}x) + \phi_{13}(\omega_{1,z}y + \omega_{1,y}z)/2 - \phi_{23}(\omega_{1,z}x + \omega_{1,x}z)/2 \end{aligned} \tag{99}$$

Combining equation (12) with Eq. (18), one gets

$$\int_{R_b'-R_b} (\mathbf{r}^{\mathrm{T}}\boldsymbol{\omega}_1 + \boldsymbol{\omega}_1^{\mathrm{T}}\mathbf{r})\mathrm{d}R = 0 \tag{100}$$

Clarifying the components of the matrix equation above, one gets

$$\int_{R_b'-R_b} \begin{bmatrix} 2\omega_{1,x}x & \omega_{1,x}y + \omega_{1,y}x & \omega_{1,x}z + \omega_{1,z}x \\ \omega_{1,x}y + \omega_{1,y}x & 2\omega_{1,y}y & \omega_{1,y}z + \omega_{1,z}y \\ \omega_{1,x}z + \omega_{1,z}x & \omega_{1,y}z + \omega_{1,z}y & 2\omega_{1,z}z \end{bmatrix} = 0 \tag{101}$$

The equation above shows that

$$\int_{R_b'-R_b} \Delta_{1,x}\mathrm{d}V = \int_{R_b'-R_b} \Delta_{1,y}\mathrm{d}V = \int_{R_b'-R_b} \Delta_{1,z}\mathrm{d}V = 0 \tag{102}$$

This means that Eq. (96) is true or Eq. (46) holds in three dimensional flow.

References

Agarwal, A.K., Jain, A.K., 2003. Dynamic behavior of offshore spar platforms under regular sea waves. Ocean Eng. 30 (4), 487–516.

Batchelor, C.K., 1967. An Introduction to Fluid Dynamics. Cambridge University Press, p. 409.

Calero, J.S., 2018. Jean Le Rond D'Alembert: A New Theory of the Resistance of Fluids. Springer International Publishing AG, p. 29.

Carbone, G., Martinat, G., Farcy, D., et al., 2019. Added masses of generic shape bodies interacting with external walls. Aerosp. Sci. Technol. 90 (JUL), 70–84.

Escareno, J., Salazar, S., Romero, H., et al., 2013. Trajectory control of a quadrotor subject to 2D wind disturbances. J. Intell. Robot. Syst. 70 (1–4), 51–63.

Faltinsen, M.O., 1990. Sea Loads on Ships and Offshore Structures. Cambridge University Press.

Fan, S., Woolsey, C.A., 2014. Dynamics of underwater gliders in currents. Ocean Eng. 84 (JUL.1), 249–258.

Hess, J.L., Smith, A., 1967. Calculation of potential flow about arbitrary bodies. Prog. Aero. Sci. 8, 1–138.

Katz, J., Plotkin, A., 2001. Low Speed Aerodynamics. Cambridge University Press, p. 63.

Kunze, E., Rosenfeld, L.K., Carter, G.S., et al., 2002. Internal waves in Monterey submarine canyon. J. Phys. Oceanogr. 32 (6), 1890–1913.

Lamb, H., 1945. Hydrodynamicsp, fifth ed. Cambridge University Press, pp. 161–162, 199.

Lin, X.W., Wang, S.C., Zhu, B., 2021. Effect of uniform incoming flow on vehicle's hydrodynamics under the same relative velocity. Ocean. Eng. available online: https://authors.elsevier.com/a/1dVyM_hNWiWkR.

Mueller, J.B., Zhao, Y.J., Garrard, W.L., 2009. Optimal ascent trajectories for stratospheric airships using wind energy. J. Guid. Control Dyn. 32 (4), 1232–1245.

Munk, M.M., 1923. Some New Aerodynamical Relations. Technical Report Archive & Image Library.

Newman, J.N., 2017. Followed by grue j marine hydrodynamics. In: The 40th Anniversary Edition, Vol. 140. the MIT Press, Londan, pp. 156–159.

Noca, F., Shiels, D., Jeon, D., 1997. Measuring instantaneous fluid dynamic forces on bodies, using only velocity fields and their derivatives. J. Fluids Struct. 11 (3), 345–350.

Noca, F., Shiels, D., Jeon, D., 1999. A comparison of methods for evaluating time-dependent fluid dynamic forces on bodies, using only velocity fields and their derivatives. J. Fluids Struct. 13 (5), 551–578.

Shen, H., Hou, Y.J., 2016. Effects of large-amplitude internal solitary waves on ROV operation-a numerical study. Sci. China : Earth Scinece 000 (005), 1074–1080.

Sun, M., 2014. Insect flight dynamics: Stability and control. Rev. Modern Phys. 86 (2), 615–646.

Taylor, G.I., 1928. The forces on a body placed in a curved or converging stream of fluid. Proc. R. Soc. Lond. 120 (785), 260–283.

Thomasson, P.G., 2000. Equations of motion of a vehicle in a moving fluid. J. Aircr. 37 (4), 630–639.

Thomasson, P.G., Woolsey, C.A., 2013. Vehicle motion in currents. IEEE J. Ocean. Eng. 38 (2), 226–242.

Thomson, W., 1872. 4. On the motion of rigid solids in a liquid circulating irrotationally through perforations in them or in any fixed solid. Proc. R. Soc. Edinb. 7, 668–682.

Wang, J., Meng, X., Li, C., 2020. Recovery trajectory optimization of the solar-powered stratospheric airship for the station-keeping mission. Acta Astronaut. 178 (3).

Woolsey, C., 2011. Vehicle Dynamics in Currents. Technical Report No. VaCAS-2011-01, Virginia Center for Autonomous Systems.

Wu, J.C., 2014:. Elements of Vorticity Aerodynamics. ShangHai JiaoTong University Press, Shanghai, p. 40.

Wu, J.Z., Ma, H.Y., Zhou, M.D., 2015. Vortical Flows. Springer, Berlin, p. 61, 107, 421-422.

Zan, X.X., Lin, Z.H.Zhenhua., 2020. On the applicability of Morison equation to force estimation induced by internal solitary wave on circular cylinder. Ocean Eng. 198, 106966.